Impacts of Major Storms on Coastal Erosion in the Texas Gulf Coast

"This report was funded by a Texas Coastal Management Program grant approved by the Texas Land Commissioner, providing financial assistance under the Coastal Zone Management Act of 1972, as amended, awarded by the National Oceanic and Atmospheric Administration (NOAA), Office for Coastal Management, pursuant to NOAA Award No. NA23NOS4190249. The views expressed herein are those of the author(s) and do not necessarily reflect the views of NOAA, the U.S. Department of Commerce, or any of their subagencies."

September 2025

Prepared by:

Shuhab Khan, Muhammad Younas, Celine Saidy, Presley Greer

Department of Earth and Atmospheric Sciences,
College of Natural Science and Mathematics, University of Houston
3507 Cullen Blvd, Houston, TX 77204
Phone No (713)743-5404
Email: sdkhan@uh.edu

Summary

Texas faces storm surges from hurricanes and tropical storms causing coastal erosion, which pose serious risks to the coastline. The sandy dunes along the Gulf Coast act as a natural barrier, providing essential protection against strong winds, waves, and storm surges. To better understand how these dunes erode and recover, this project was designed to monitor six locations along the Texas coast, specifically on different barrier islands. The sites we chose are West Galveston Island, Follet Island, Sargent Beach, Matagorda Peninsula, Mustang Island, and North Padre Island.

We aimed to measure how much sediments are lost or gained at these locations by using drone technology to capture images and data every six months. Our main goal was to observe how erosion occurs and how the dunes recover after hurricanes or tropical storms. Originally, we planned to conduct three surveys at these sites in December 2023, May 2024, and December 2024. However, after Hurricane Beryl hit the Texas coast in July 2024, we conducted an additional survey. We ended up performing four surveys in total: December 2023, May 2024, July/August 2024, and May/June 2025.

Our studies, before and after the hurricane, revealed significant changes in the dune systems. For instance, we found that Sargent Beach experienced extensive damage, leading to the destruction of most dunes. Follet Island had some restoration but still lost a substantial amount of sand. West Galveston Island suffered damage to its coppice dunes, while Matagorda Peninsula saw only minor changes. Mustang Island and North Padre Island also experienced some erosion, but less so than Sargent Beach and Follet Island, mainly due to their higher dunes and better vegetation.

This research shows how local conditions and storm surges can vary greatly in their impact on coastal erosion. Our findings were published in a scientific paper and received attention from various media outlets. Additionally, we created an interactive website to share the results of our study with the public.

Table of Contents

List of Tables

List of Figures

1. Introduction

Sand dunes are a prevalent feature of the Texas coastline. They provide habitat for animals and plants as well as nesting grounds for migratory birds. Dunes also protect the inland areas from storm surges or sea intrusions (Fabbri et al., 2021). The Texas coastal zone is one of the most dynamic environments in the country (Finley, 1976; Paine et al., 2013). It is constantly being altered by erosion and accretion from storms, as well as natural biogenic and anthropogenic processes. Erosion and shoreline retreat are the primary contributors to land loss in this region (Morton and Paine, 1990). According to the Texas General Land Office, for 367 miles of the Texas coast, the average erosion rate of the shoreline is 4.1ft/year, and 80% of the Texas coast is classified as critically eroded. As the amount of sediment available on the beach increases and decreases with storms and outwash events, beach dunes also grow and shrink. This affects their ability to protect the inland from storm damage. As beach and dune characteristics are different along the Texas coast, it is important to determine the characteristics of each area.

The presence of vegetation is one of the most important factors in building dunes and stabilizing barrier islands. Aboveground plant biomass has been shown to reduce erosion on high energy beaches (Feagin et al., 2019). This is due to attenuating wave energy, which plays a significant role in reducing the wave energy during storm surges. The coverage of vegetation will lead to dune stabilization, where the dune is no longer mobile or active (Tsoar, 2005). In addition to trapping windblown sand, plants can transform the nature of the sand by adding organic matter, increasing clay content with trapped fine sediment, and providing shade that helps retain moisture, all of which tend to increase cohesion and reduce erodibility (Feagin et al., 2015). Many species of plants living in barrier-island eco systems are adapted to storm events: marsh grass, for instance, increases growth rates when buried in sand up to an optimal depth (Baustian & Mendelssohn, 2015; Feagin et al., 2015; Maun, 1998; McKee & Cherry, 2009; Walters &Kirwan, 2016).

Tropical storms and hurricanes are among the most dangerous and financially devastating natural disasters impacting the Gulf Coast states of the United States. The Texas coast alone has experienced 109 hurricanes and tropical storms since 1850 (NOAA, 2024). Research shows that, on average, the intensity, frequency, and resulting damage from tropical storms have increased over time (Holland and Webster, 2007; Hallam et al., 2019). In addition to property damage and flooding, hurricanes and tropical storms also play a role in the erosion of beaches and dunes. Wave strength or high energy waves, regarding strong storm surges cause erosion of dunes and shoreline (Feagin et al., 2019). Previous studies have shown that hurricanes such as Hurricane Harvey have caused drastic beach-dune erosion and shoreline retreat along Texas barrier islands (Shahtakhtinskiy et al., 2023, Rojas et al., 2022). Tropical storms and hurricanes also decimate coastal vegetation, leaving beaches and dunes even more vulnerable to further erosion after the storm (Over and Sherwood, 2025).

2. Methods

2.1. Data Acquisition

The six study sites are located on Follet Island, Galveston Island, Matagorda Bay, Mustang Island, North Padre Island, and Sargent Island (Figure 1). Data collection using drones began in December 2023 and was initially planned to occur every six months. However, after Hurricane Beryl made landfall in Matagorda, Texas, as a Category 1 storm on July 8, 2024, drone surveys were conducted 17 days later to assess and quantify the hurricane's impact on the shoreline. In total, drone surveys at each site were conducted four times: December 2023, May 2024, July 2024, and May 2025.

The data acquired in surveys include three different types of data. The first are RGB photos from a high-resolution camera. The second is LiDAR using L1 sensor. Both were used for topographic surveys, to create DEMs. The third type is multispectral data. It collects spectral information within four bands. This includes bands in green, red, red edge, and near infrared wavelengths.

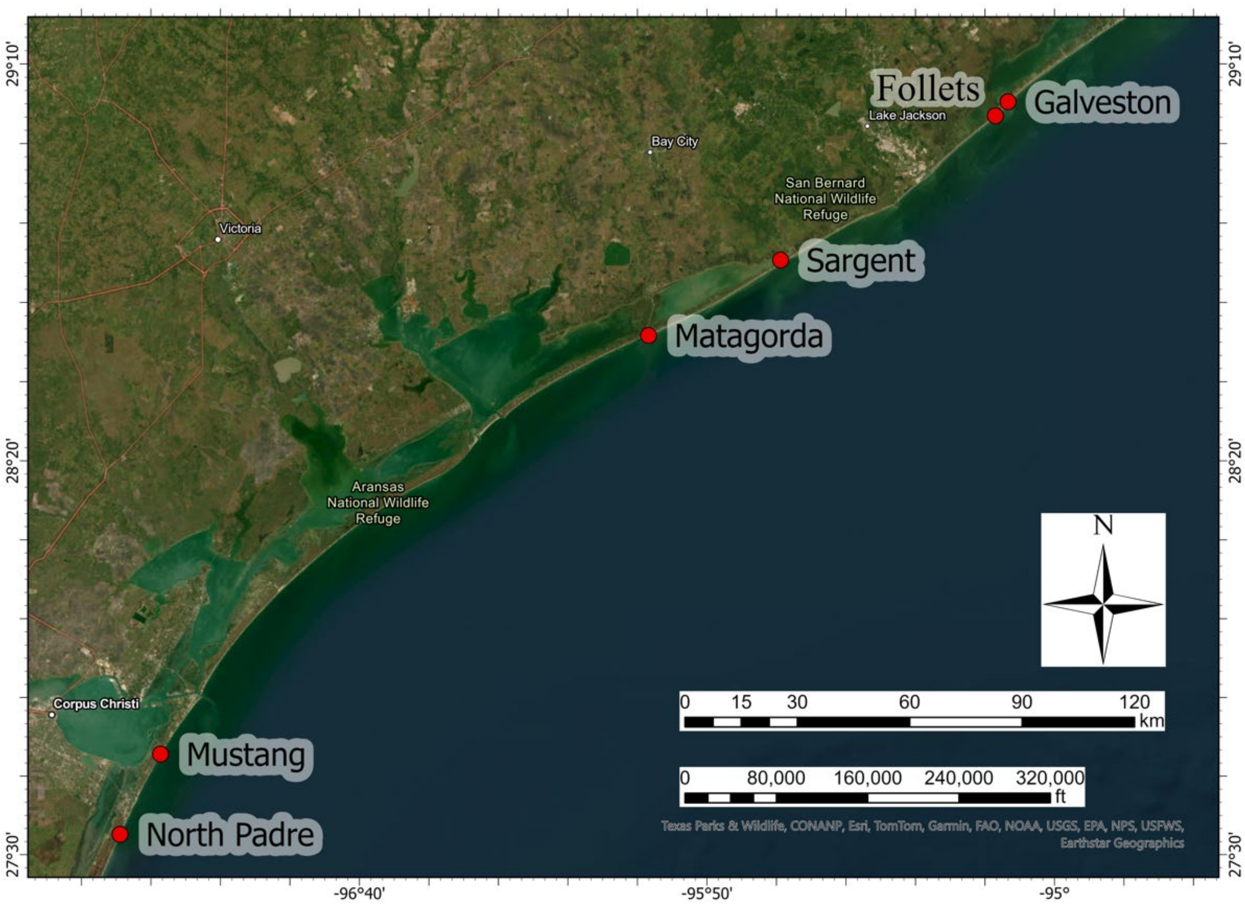

Figure 1. Map showing six study sites from northeast to southwest. These include Galveston Island, Follet Island, Sargent Beach, Matagorda Peninsula, Mustang Island and North Padre Island.

The drone data sets were collected by the University of Houston GeoRS (Geospatial and Remote Sensing) lab. Survey plans were created to be able to capture the foredunes and shorelines of study sites. Ground control points (GCPs) were laid out in a random orientation of varying elevations. Using global navigation satellite system (GNSS) receivers, data consisting of longitude, latitude, and elevation were collected at the center of each GCP (Figure 2). This GNSS data was then further corrected using permanent GPS CORS stations to create highly accurate post-processed kinematic data (PPK). This PPK data was used during processing that uses geometry to obtain elevation from images (photogrammetry), and during the processing of LiDAR data.

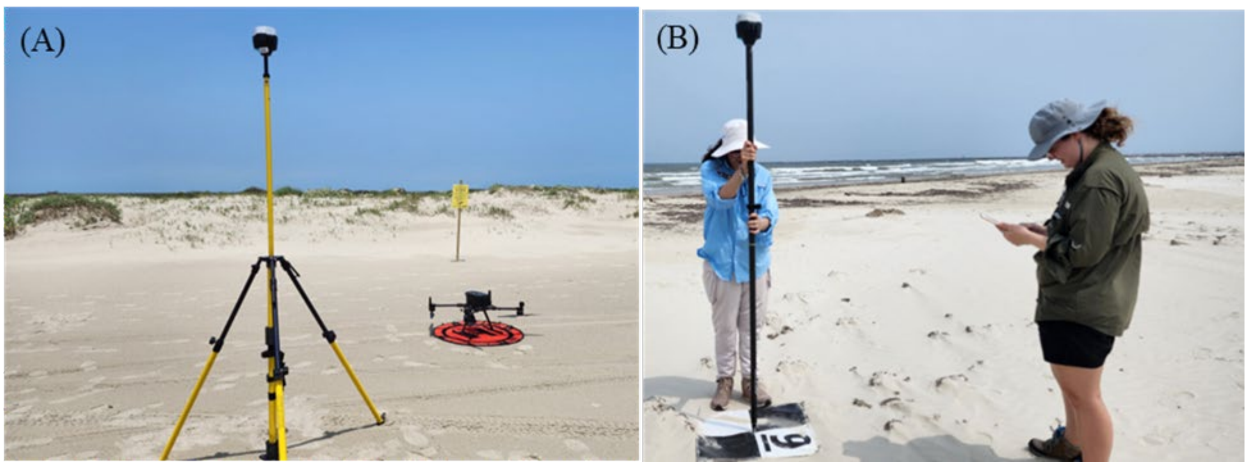

Figure 2. Equipment used during drone surveys. (A) Emlid Reach local base station setup (left) and drone with Lidar (right). (B) Emlid Reach rover stop-and-go method of data collection at ground control points.

2.2. Data Analysis

The GNSS data collected during the drone surveys were crucial during the photogrammetry image processing to obtain elevation, as well as during LiDAR data processing. Drone2Map software was utilized to mosaic the RGB images by stitching them together using tie points. LiDAR data was processed with Terra software, while the multispectral data using PIX4D Fields software. The GNSS data enhanced the accuracy of the mosaiced images and served as a validation check on the output DEMs at the GCP locations. The DEMs were created using the EGM2008 geoid to calculate orthometric heights from the ellipsoidal heights.

Cross-sectional elevation profiles were generated using the interactive elevation profile creation methods available in ArcGIS Pro. These profiles were exported into Microsoft Excel. The elevation profiles of the same transect over time were arranged on the same graph. For further elevation analysis in ArcGIS Pro, change maps, which illustrate areas of erosion and deposition between two consecutive surveys, were generated by subtracting the older DEM raster from the newer one. Thus, DEM differencing was utilized to identify areas experiencing net vertical erosion (indicated by a negative elevation difference) and/or deposition (indicated by a positive elevation difference). Volume changes between surveys were calculated for both entire site areas and foredune complex areas using the cut/fill geoprocessing tool in ArcGIS Pro. For the multispectral imagery, individual band images from the sensor data were combined into an orthomosaic for each site using PIX4D, achieving a resolution of 4 cm. These orthomosaics were utilized to generate the Normalized Difference Vegetation Index (NDVI). NDVI was classified into four classes corresponding to no vegetation, sparse vegetation, moderate vegetation, and dense vegetation. Raster calculations were employed to analyze changes between the NDVI maps.

3. Results

This work resulted in several outcomes: 1) Time series DEM and orthomosaic showing changes in elevation and morphology, 2) Time series maps showing changes in vegetation, 3) A dedicated interactive website showing DEM and orthomosaic for each site, and 4) Publications/thesis. Below, we provided a summary of these products

3.1. Time Series Maps of Dunes

3.1.1. Galveston

A DEM image of Galveston taken in June 2025 is shown in Figure 3. It depicts the dunes' horizontal and vertical positions. Elevation profiles created using DEM data from December 2023, May 2024, July 2024, and June 2025 are shown in Figures 4 and 5 are indicated by two red lines on Figure 3.

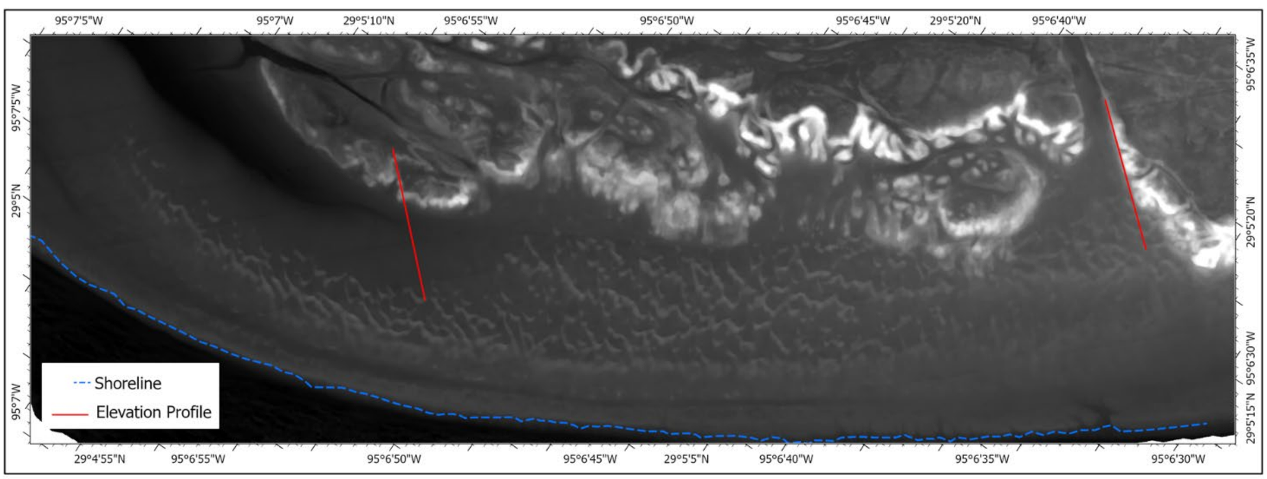

Figure 3. Map depicting the location of profiles and shoreline on DEM image of June 2025. The red line represents location of elevation profiles shown in Figures 4 and 5.

The left transect in Figure 4 indicates that elevations were highest in May 2024, but these areas were eroded by Hurricane Beryl. The profile observed in July 2025 shows that the foredunes appear to be rebuilding, although they have shifted slightly landward. The right transect of elevation profiles shown in Figure 5 indicates that the highest elevation was recorded in May 2024. The most recent DEM, as of June 2025, shows recovery after erosion by Hurricane Beryl in July 2024.

Figure 6 illustrates the change in elevation between December 2023 and May 2024, indicating an increase in elevation across all areas. Figure 7 highlights the effects of Hurricane Beryl on the foredune ridge and the interdunal troughs, demonstrating both erosion and deposition on the beach. The DEM difference between July 2024 and June 2025 shows the recovery and repositioning of sand in areas that were eroded by the hurricane (Figure 8).

Table 1 summarizes the changes in sediment volume. The net volume change between December 2023 and May 2024 is estimated to be 109782 cubic meters of sediment gain. From May 2024 to July 2024, there is an overall gain of 5,396 cubic meters. However, between July 2024 and June 2025, there is a net loss of 9,194 cubic meters of sediment.

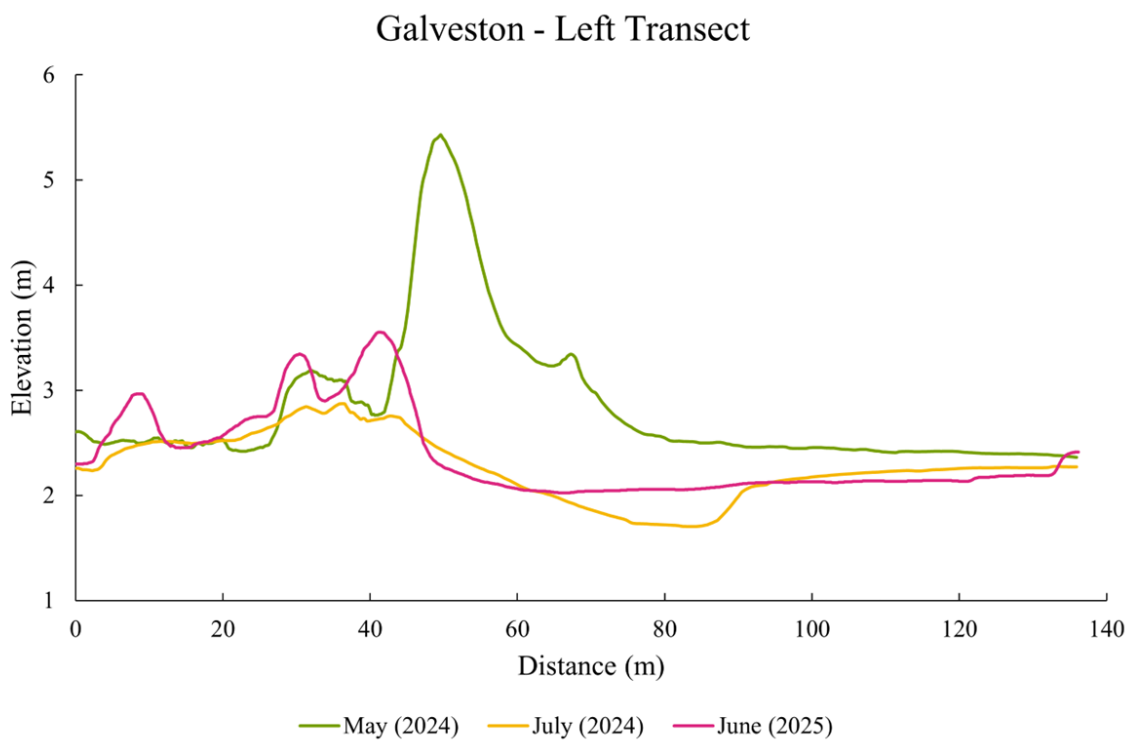

Figure 4. Elevation profiles for Galveston showing changes in elevation of dunes for three DEMs collected in May 2024, July 2024, and June 2025. Location of profile shown in Figure 3.

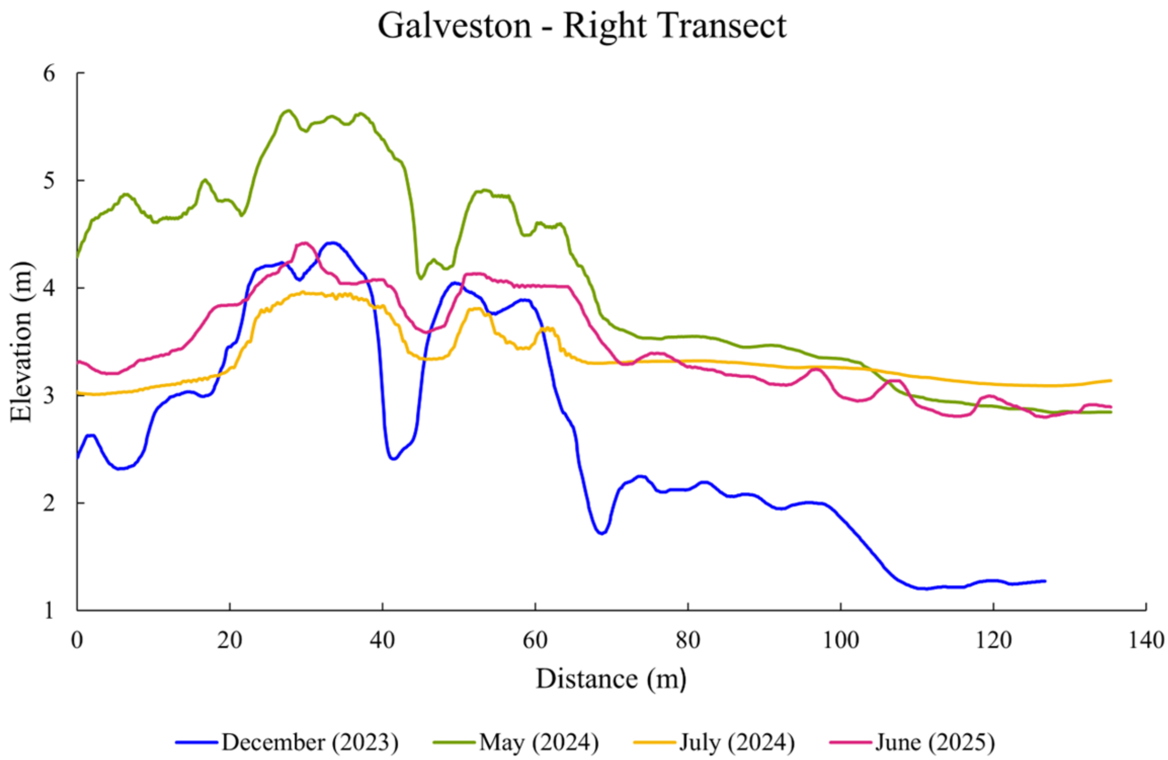

Figure 5. Elevation profiles for Galveston showing changes in elevation of dunes for four DEMs collected in December 2023, May 2024, July 2024, and June 2025. Location of profile shown in Figure 3.

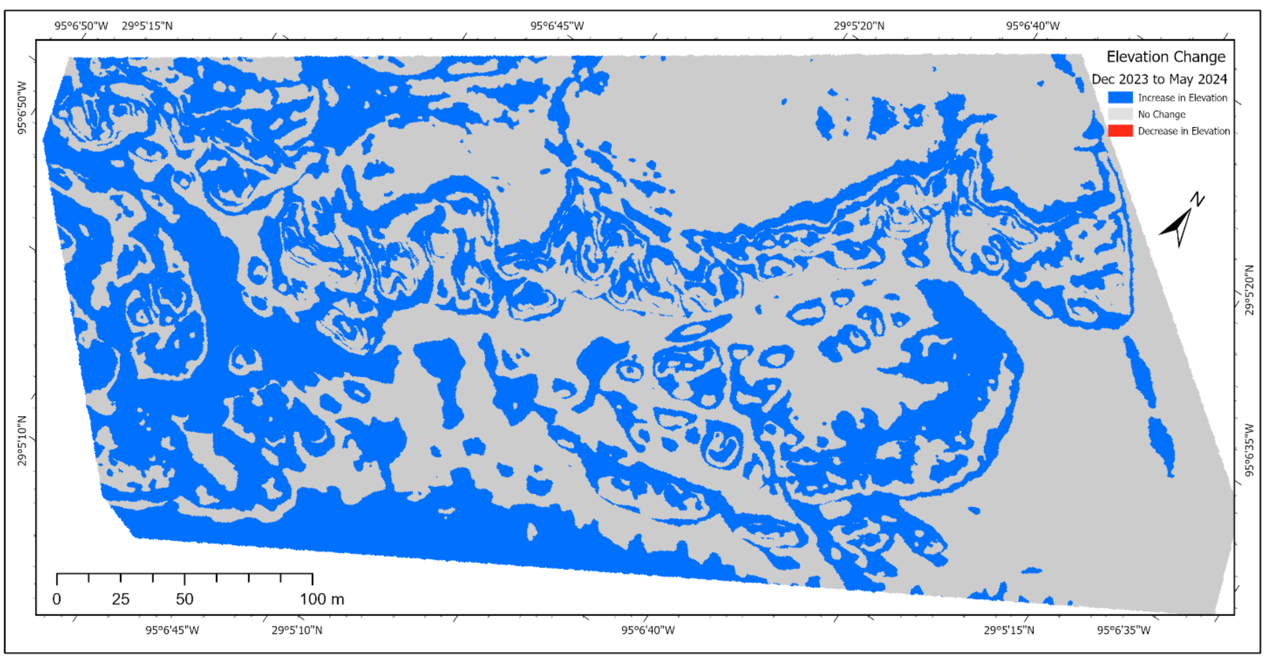

Figure 6. Map of elevation changes between December 2023 and May 2024 for Galveston.

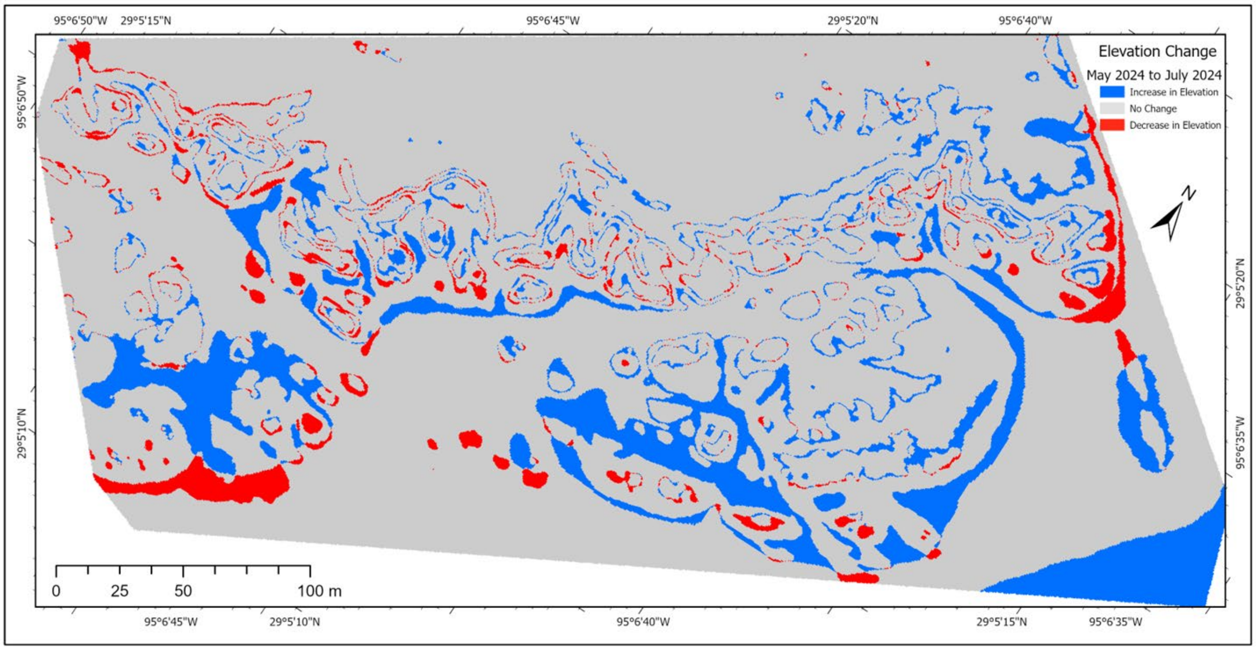

Figure 7. Map of elevation changes between May 2024 and July 2024 for Galveston.

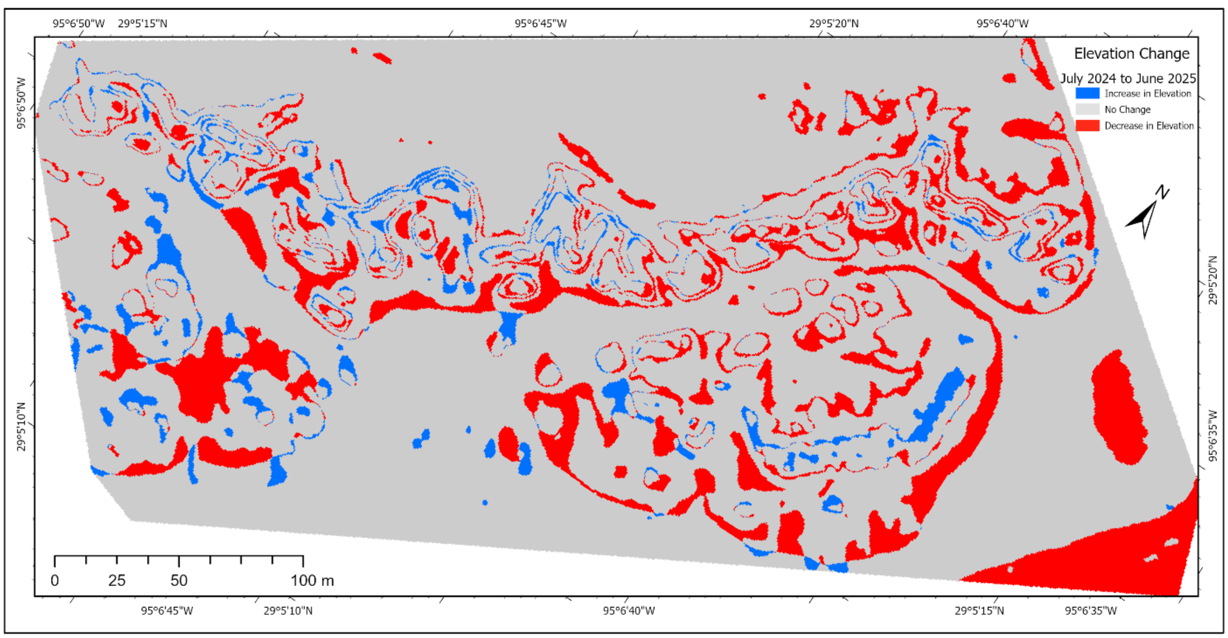

Figure 8. Map of elevation changes between July 2024 and June 2025 for Galveston.

Table 1. Summary of Sediment Volume Change for Galveston.

Galveston	**December 2023 to May 2024**	**May 2024 to July 2024**	**July 2024 to June 2025**
Net Gain (m^3)	-109842.6	-8453.8	-2484.9
Net Loss (m^3)	60.5	3057.8	11678.8
Net Change (m^3)	-109782.1	-5395.9	9194.0
Site Area (m^2)	78098.5	78070.5	78050.3

3.1.2. Follet Island

Figure 9 illustrates a DEM image of Follet, obtained on June 2025. It displays the vertical and horizontal positions of the dunes. Two red lines on Figure 9 represent the sites of elevation profiles developed using DEM data from December 2023, May 2024, July 2024, and June 2025 and displayed in Figures 10 and 11. The left transect in Figure 10 illustrates that elevations were highest in December 2023 and May 2024, but these areas were eroded by Hurricane Beryl. The profile recorded in June 2025 shows some recovery. Figure 11's right transect of elevation profiles displays the highest elevation in December 2023. The most recent DEM demonstrates recovery following Hurricane Beryl's erosion in July 2024.

The change in elevation from December 2023 to May 2024 is shown in Figure 12, which indicates an increase in elevation on the beach, along with some erosion in the back dune area. Figure 13 illustrates the impact of Hurricane Beryl on the region, highlighting significant erosion affecting both the beach and dunes. Additionally, the DEM difference between July 2024 and May 2025 depicts some recovery and reshaping in the areas that were eroded by the hurricane. (Figure 14).

The sediment volume changes are summarized in Table 2. It is estimated that there is a net volume change of 2,759 cubic meters of sediment between December 2023 and May 2024. 11,234 cubic meters are lost between May and July of 2024. Finally, there is a net increase of 2,938 cubic meters of sediment between July 2024 and June 2025.

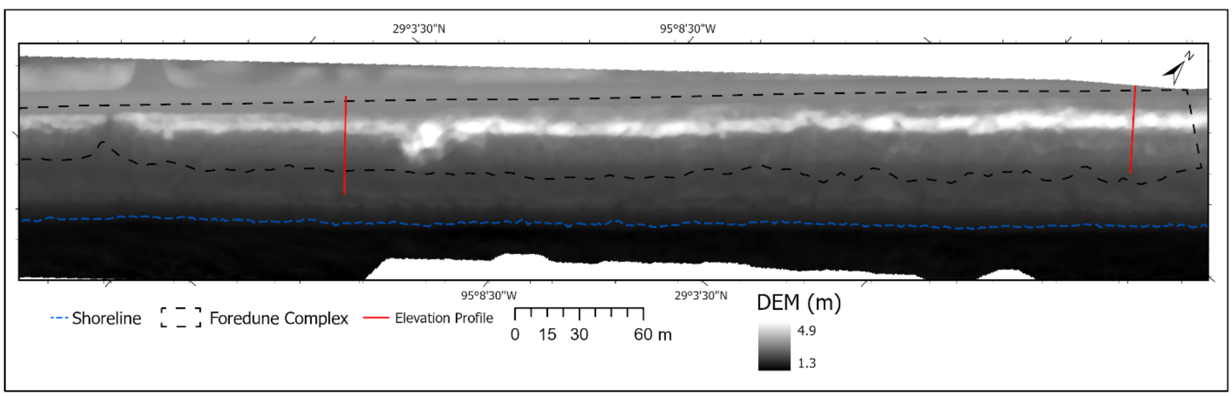

Figure 9. Map depicting the location of profiles and shoreline as of June 2025, DEM. The red line represents the profiles used to create the elevation profiles shown in Figures 10 and 11.

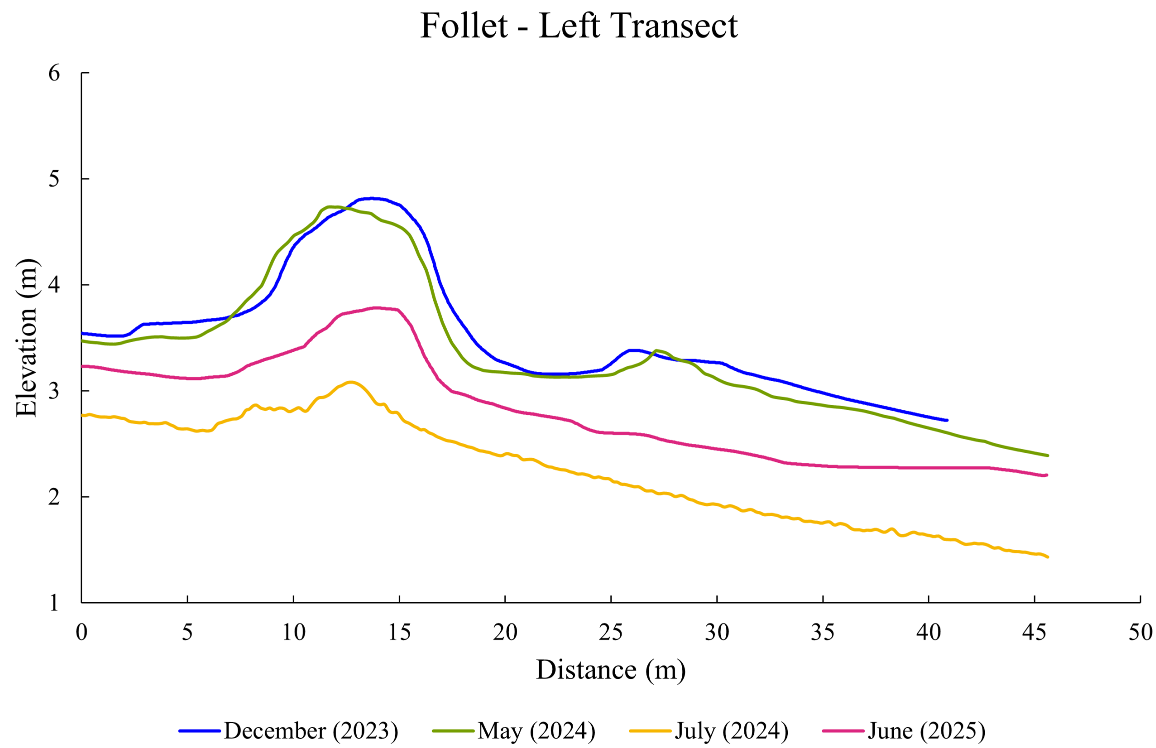

Figure 10. Elevation profiles for Follet showing changes in elevation of dunes for three DEMs collected in May 20024, July 2024, and June 2025. Location of profile shown in Figure 9.

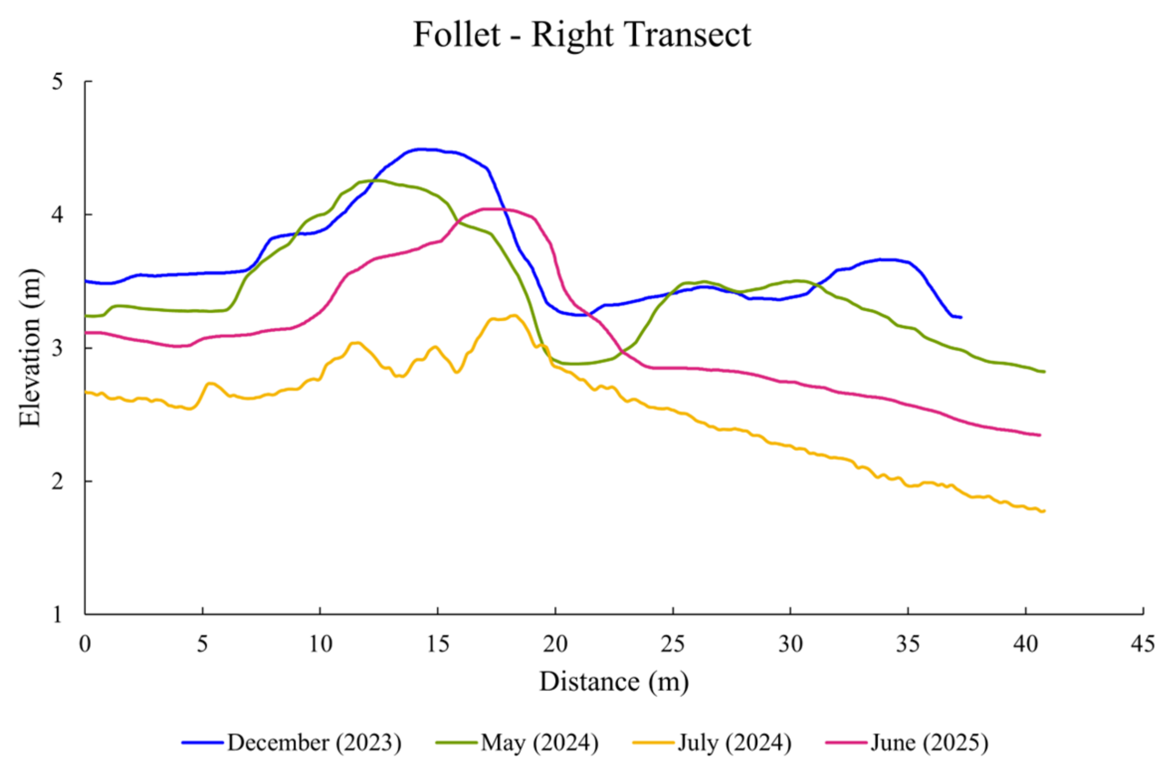

Figure 11. Elevation profiles for Follet showing changes in elevation of dunes for three DEMs collected in May 20024, July 2024, and June 2025. Location of profile shown in Figure 9.

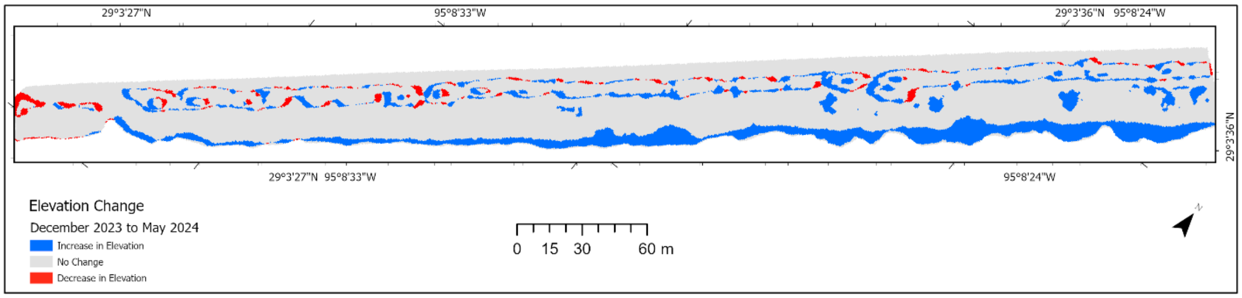

Figure 12. Map of elevation changes between December 2023 and May 2024 for Follet.

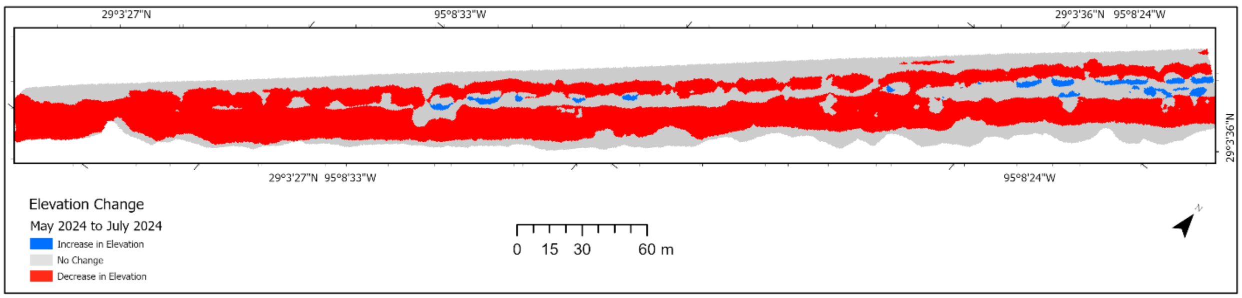

Figure 13. Map of elevation changes between May 2024 and July 2024 for Follet.

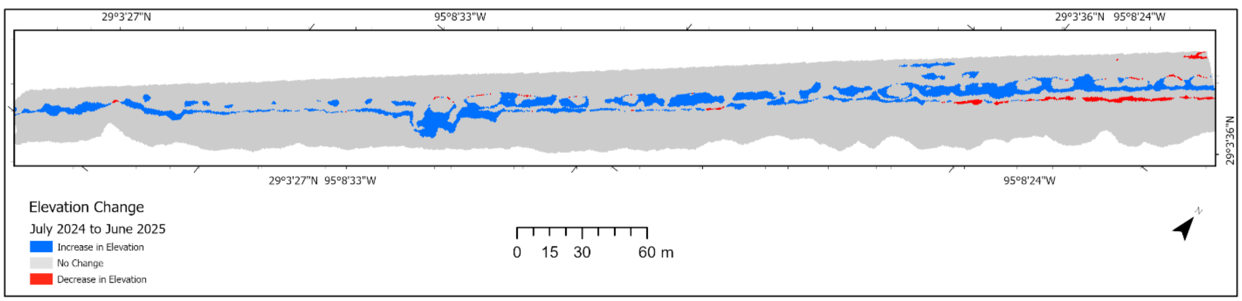

Figure 14. The elevation changes between July 2024 and June 2025 for Follet.

Table 2. Summary of Volume Change for Follet.

Follet	**December 2023 to May 2024**	**May 2024 to July 2024**	**July 2024 to June 2025**
Net Gain (m^3)	-583.6	-295.2	-3104.4
Net Loss (m^3)	3342.3	11529.4	166.1
Net Change (m^3)	2758.7	11234.2	-2938.3
Site Area (m^2)	19152.1	19200.5	19192.7

3.1.3. Sargent Beach

A DEM image of Sargent collected in June 2025 is shown in Figure 15. It depicts the dunes' horizontal and vertical positions. The locations of elevation profiles produced using DEM data from December 2023, May 2024, August 2024, and June 2025, and shown in Figures 16 and 17, are indicated by two red lines on Figure 15. Elevations peaked in May 2024, as seen by the left transect in Figure 16, but Hurricane Beryl eroded these places. Although the dunes have eroded significantly, the profile in June 2025 indicates that there seems to be rebuilding. Figure 17's right transect of elevation profiles displays the highest elevation in June 2025 and shows recovery following Hurricane Beryl's erosion in July 2024.

The elevation shifts between December 2023 and May 2024 are depicted in Figure 18, which shows a decrease in elevation in the area. Figure 19 illustrates how Hurricane Beryl affected the beach and dunes showing both beach erosion and redeposition. Recovery in hurricane-eroded areas are depicted in the DEM difference between August 2024 and June 2025 (Figure 20).

The variations in sediment volume are compiled in Table 3. It is estimated that there is a net volume change of 27,636 cubic meters of sediment loss between December 2023 and May 2024. The total gain from May 2024 to August 2024 is 69,282 cubic meters. However, there is an overall gain of 22,631 cubic meters of sediment between July 2024 and June 2025.

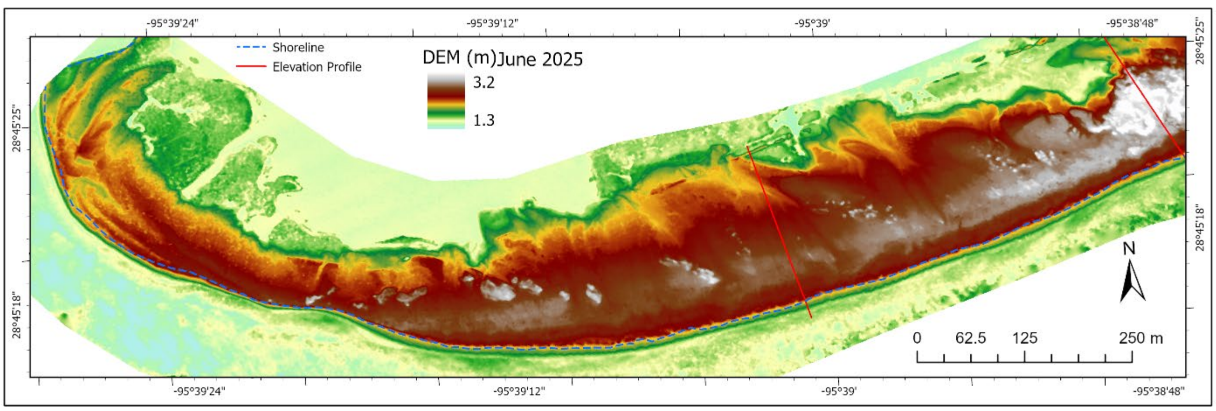

Figure 15. Map depicting the location of profiles and shoreline as of June 2025, DEM. The red line represents the profiles used to create the elevation profiles shown in Figures 16 and 17.

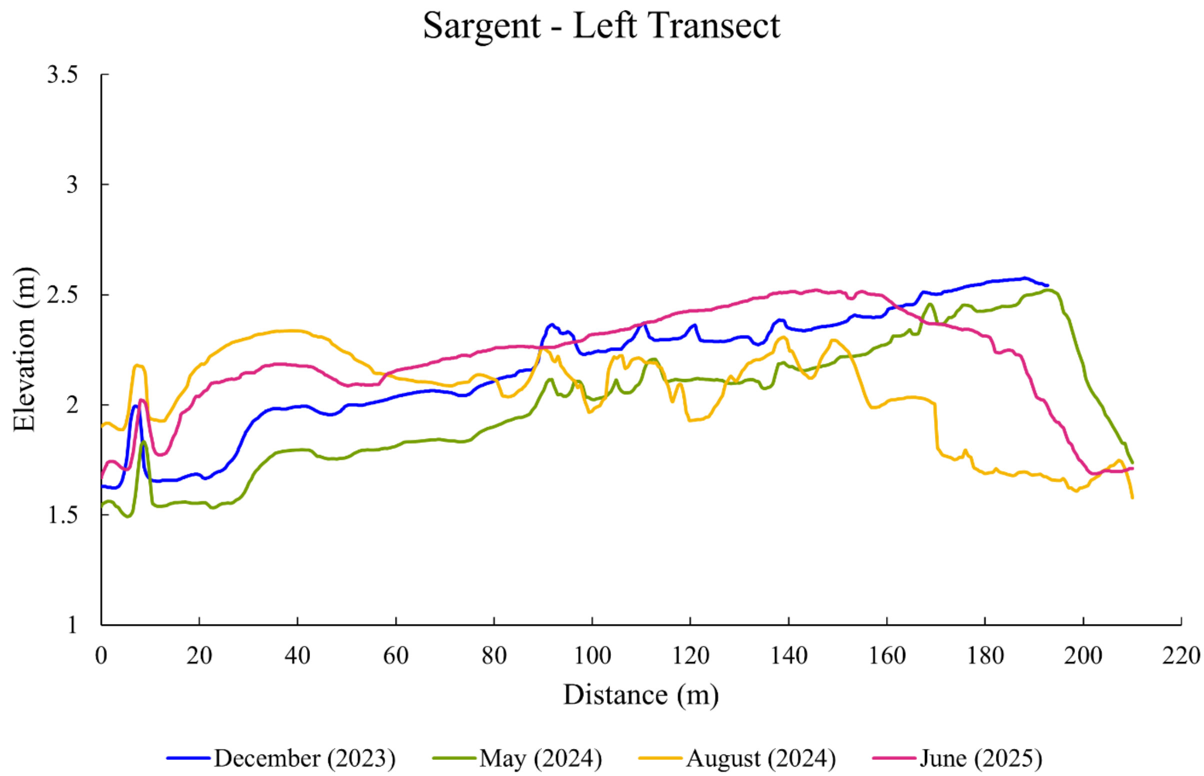

Figure 16. Elevation profiles for Sargent showing changes in elevation of dunes for four DEMs collected in December 2023, May 2024, August 2024, and June 2025. Location of profile shown in Figure 15.

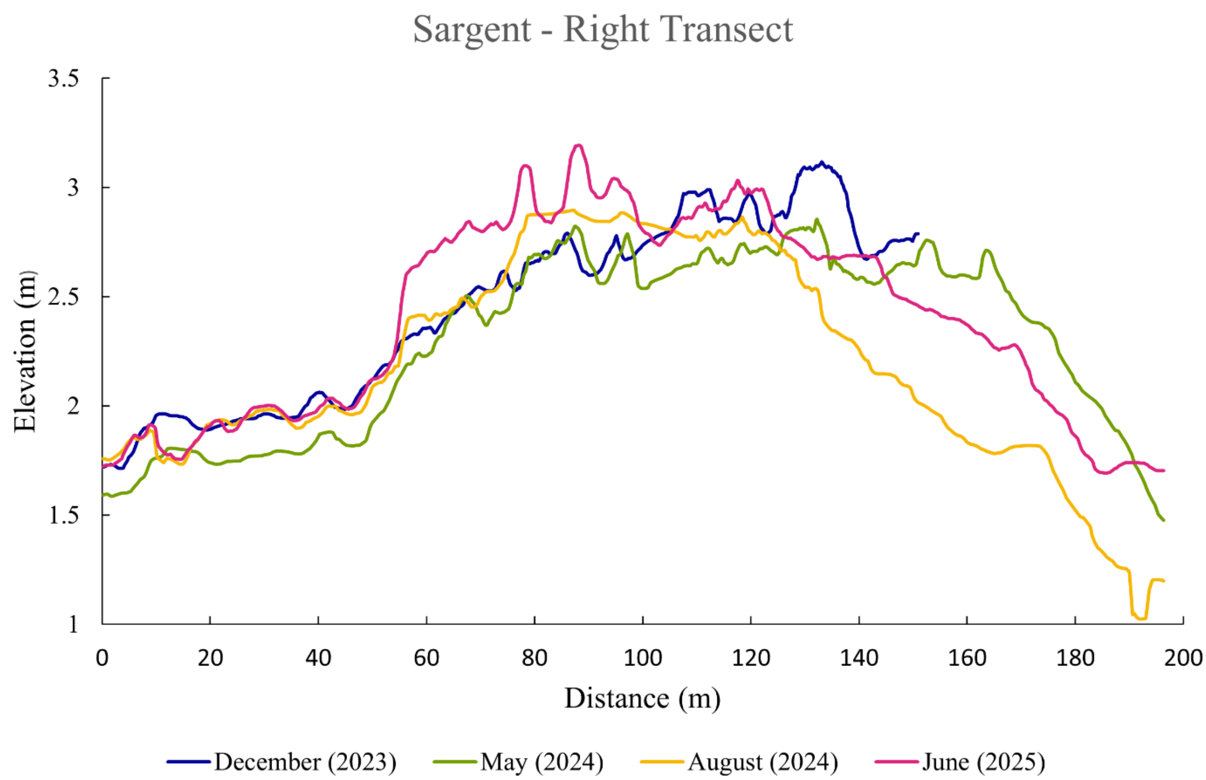

Figure 17. Elevation profiles for Follet showing changes in elevation of dunes for four DEMs collected in December 2023, May 2024, August 2024, and June 2025. Location of profile shown in Figure 15.

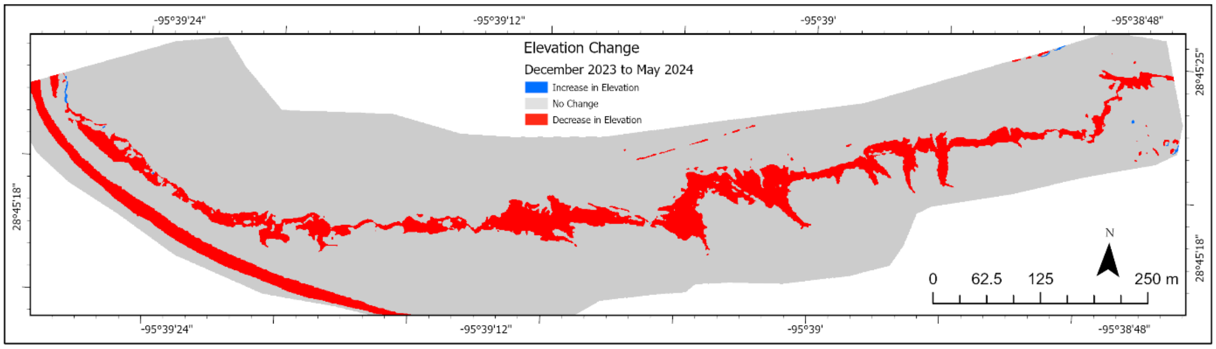

Figure 18. The elevation changes between December 2023 and May 2024 for Sargent.

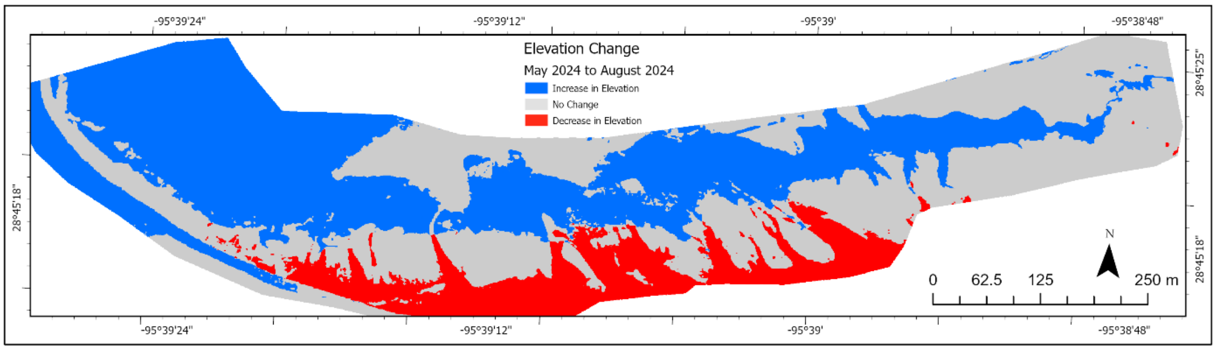

Figure 19. The elevation changes between May 2024 and August 2024 for Sargent.

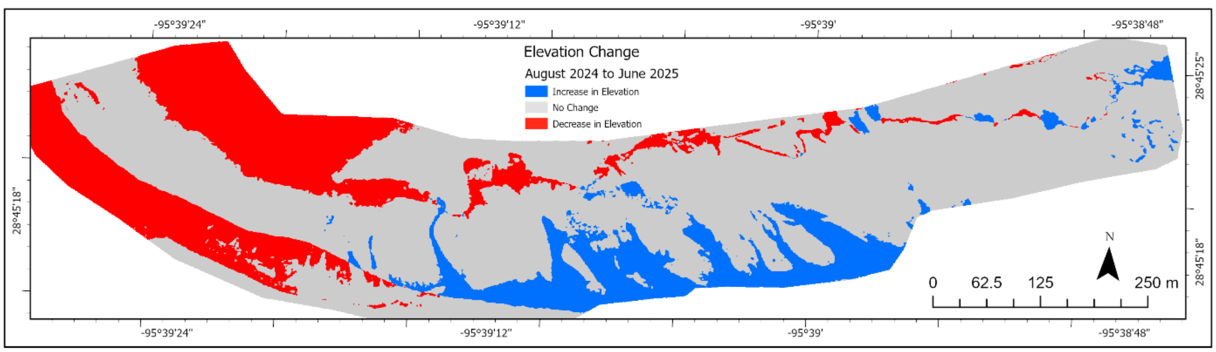

Figure 20. Map of elevation changes between August 2024 and June 2025 for Sargent.

Table 3. Summary of Volume Change for Sargant.

Follet	**December 2023 to May 2024**	**May 2024 to July 2024**	**July 2024 to June 2025**
Net Gain (m^3)	-123.8	-98920.6	-25765.4
Net Loss (m^3)	27759.3	29638.8	48396.2
Net Change (m^3)	27635.5	-69281.7	-22630.9
Site Area (m^2)	227093.3	227320.4	227320.4

3.1.4. Matagorda Peninsula

Figure 21 displays a DEM image of Matagorda, collected in May 2025. It illustrates the vertical and horizontal positions of the dunes. Two red lines on Figure 21 indicate the locations of elevation profiles generated using DEM data from December 2023, May 2024, July 2024, and June 2025 and displayed in Figures 22 and 23.

The left transect in Figure 22 indicates that elevations were slightly higher in May 2024 at foredunes and show some erosion by Hurricane Beryl. The profile observed in July 2025 shows that the foredunes appear to be rebuilt with a slight shift. The right transect of elevation profiles shown in Figure 23 reveals minimal change at the foredunes, but a higher elevation at the back dunes following Hurricane Beryl, which has decreased in the most recent DEM of May 2025.

Figure 24 illustrates the change in elevation between December 2023 and May 2024, indicating an increase in elevation across all areas. Figure 25 highlights the effects of Hurricane Beryl on the foredune ridge and shows deposition on the beach and back dunes area. The DEM difference between July 2024 and May 2025 shows recovery in foredunes and loss of sediment in back dunes and on the beach (Figure 26).

Table 4 summarizes the changes in sediment volume. The net volume change between December 2023 and May 2024 is estimated to be 13,302 cubic meters of sediment gain. From May 2024 to July 2024, there is a total increase in sediment of 22,877 cubic meters, and between July 2024 and June 2025, there is anof 34,538 cubic meters of sediment.

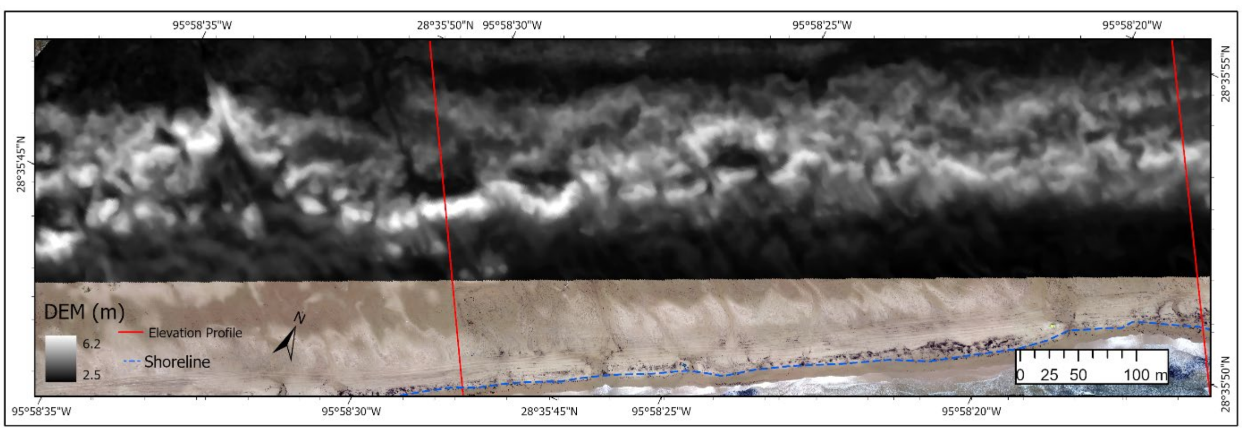

Figure 21. Map depicting the location of profiles and shoreline as of May 2025, DEM. The red line represents the profiles used to create the elevation profiles shown in Figures 22 and 23.

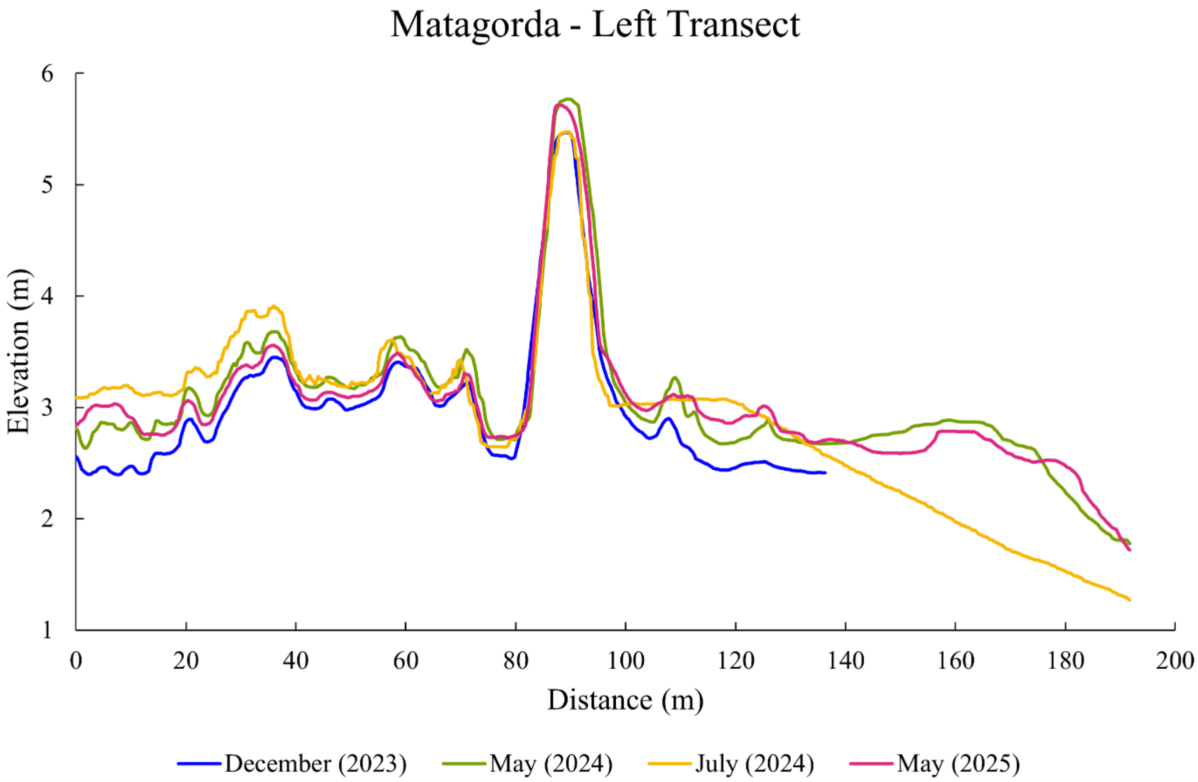

Figure 22. Elevation profiles for Matagorda showing changes in elevation of dunes for four DEMs collected in December 2023, May 2024, July 2024, and May 2025. Location of profile shown in Figure 21.

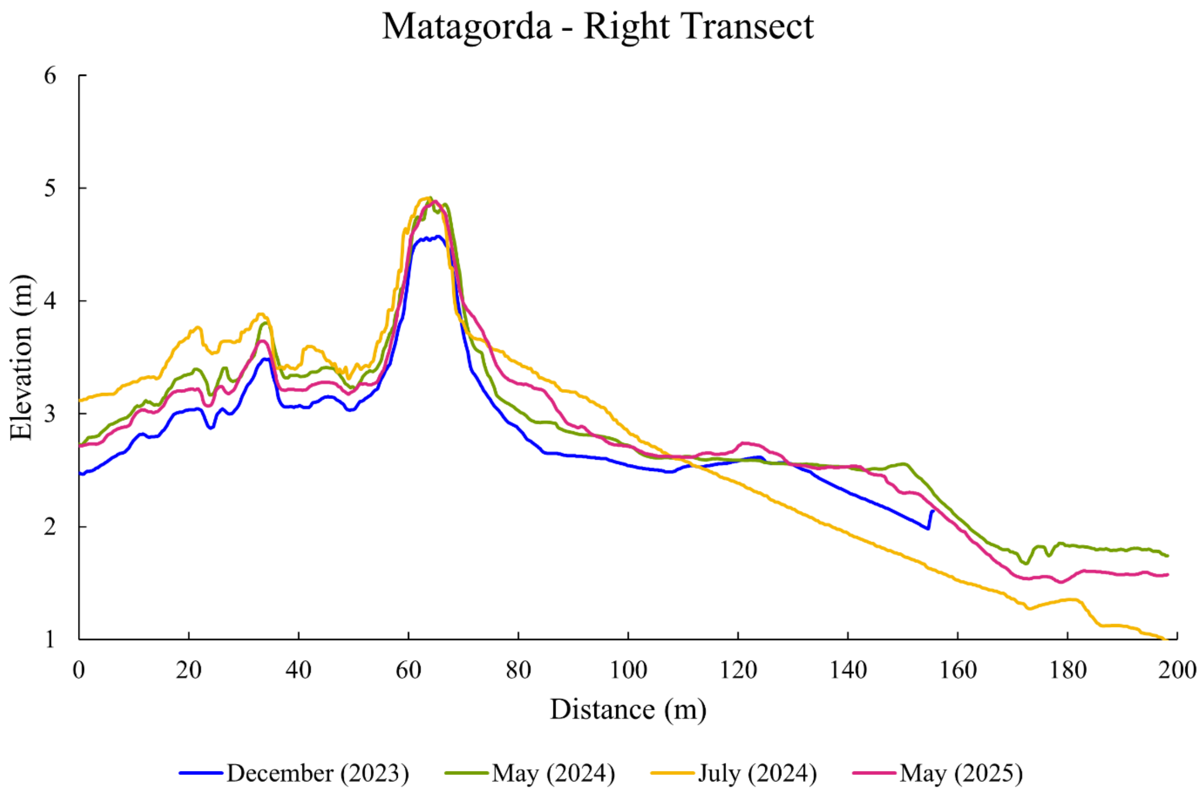

Figure 23. Elevation profiles for Matagorda showing changes in elevation of dunes for four DEMs collected in December 2023, May 2024, July 2024, and May 2025. Location of profile shown in Figure 21.

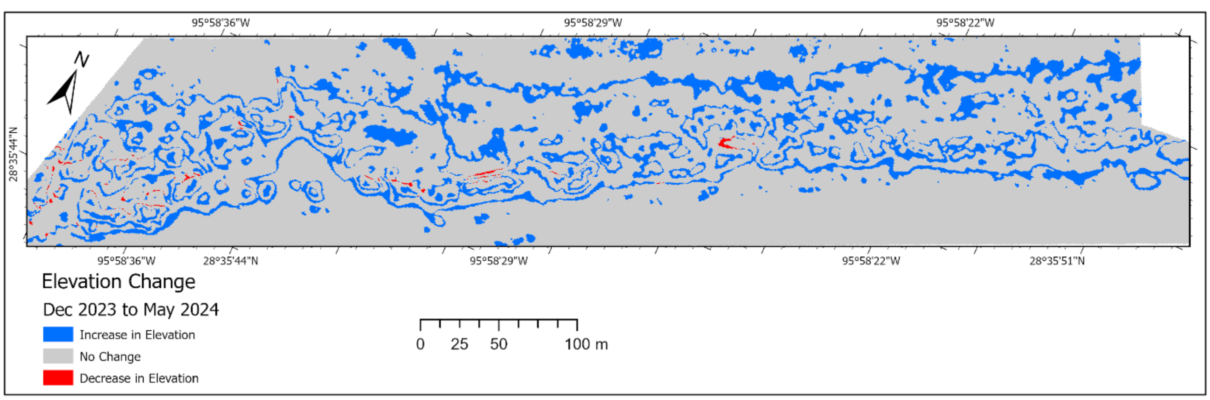

Figure 24. Map of elevation changes between December 2023 and May 2024 for Matagorda.

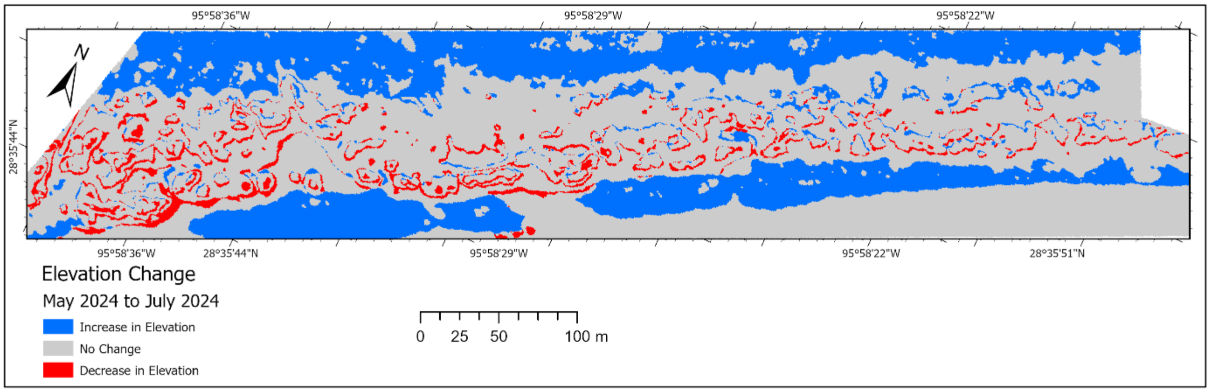

Figure 25. Map of elevation changes between May 2024 and July 2024 for Matagorda.

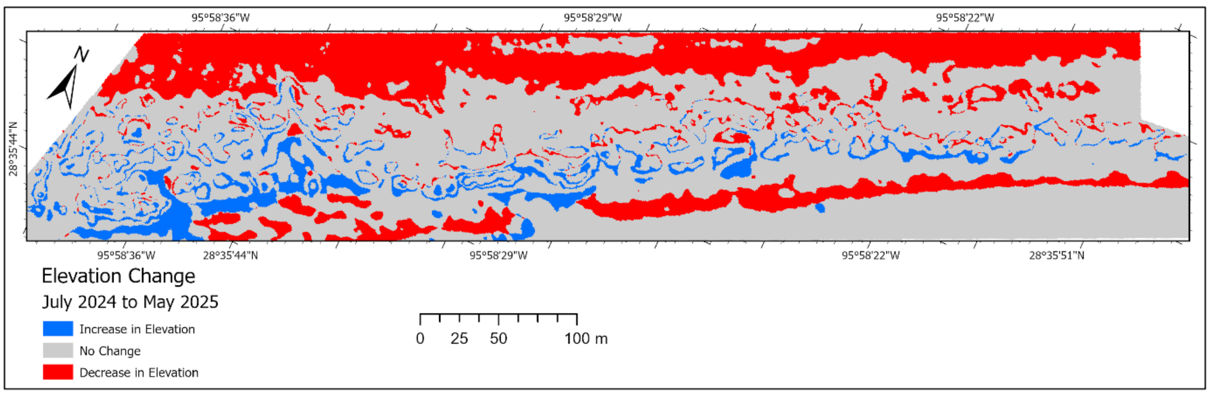

Figure 26. Map of elevation changes between July 2024 and May 2025 for Matagorda.

Table 4. Summary of Volume Change for Matagorda.

Matagorda	**December 2023 to May 2024**	**May 2024 to July 2024**	**July 2024 to June 2025**
Net Gain (m^3)	-13464.0	-27198.8	-38496.5
Net Loss (m^3)	162.3	4322	3958.3
Net Change (m^3)	-13301.8	-22876.8	-34538.2
Site Area (m^2)	89730.0	89680.3	89725.5

3.1.5. Mustang Island

A DEM image of Mustang Island taken in June 2025 is shown in Figure 27. It depicts the dunes' horizontal and vertical positions. The locations of elevation profiles produced using DEM data from December 2023, May 2024, July 2024, and June 2025, and shown in Figures 28 and 29, are indicated by two red lines on Figure 27. The elevations were highest in December 2023 and lowest in July 2024 after Hurricane Beryl, and the most recent data shows recovery of foredunes as shown by the elevation profiles shown in Figures 28 and 29.

The elevation change from December 2023 to May 2024 is shown in Figure 30, which shows that the elevation decreased at the beach and a few other places in foredunes and back dunes, while other areas gained elevation. Figure 31 illustrates that Hurricane Beryl affected the entire area and the overall elevation decreased. Recovery and deposition of sediments are depicted in the DEM difference between July 2024 and May 2025 (Figure 32).

A summary of the sediment volume variations is provided in Table 5. It is estimated that there is a net volume change of 3,909 cubic meters of sediment loss between December 2023 and May 2024. The overall loss from May 2024 to July 2024 is 23,085 cubic meters. However, there is a net gain of 11,117 cubic meters of sediment between July 2024 and June 2025.

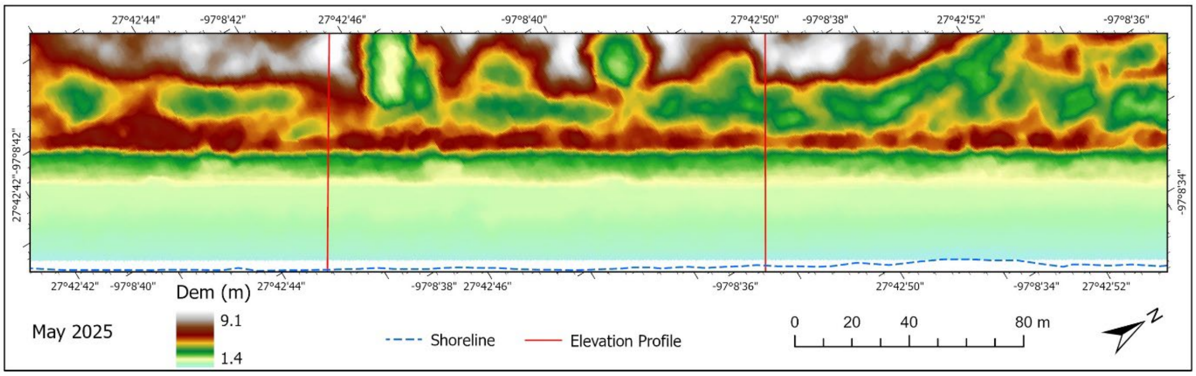

Figure 27. Map depicting the location of profiles and shoreline as of May 2025, DEM. The red line represents the profiles used to create the elevation profiles shown in Figures 28 and 29.

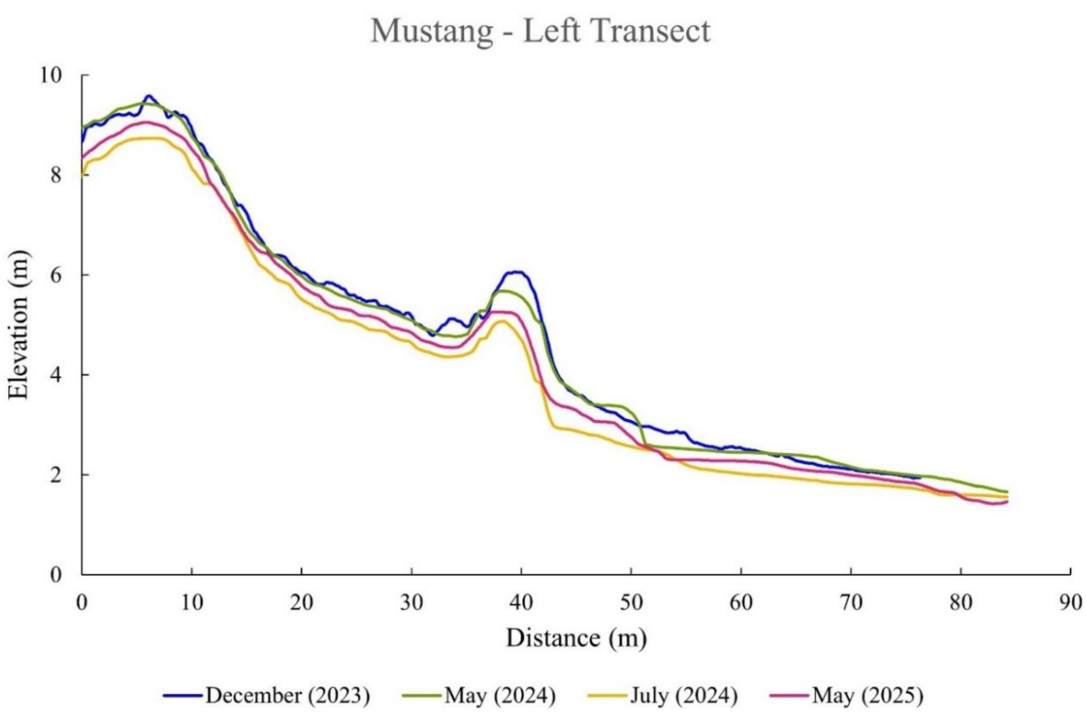

Figure 28. Elevation profiles for Mustang showing changes in elevation of dunes for four DEMs collected in December 2023, May 2024, July 2024, and May 2025. Location of profile shown in Figure 27.

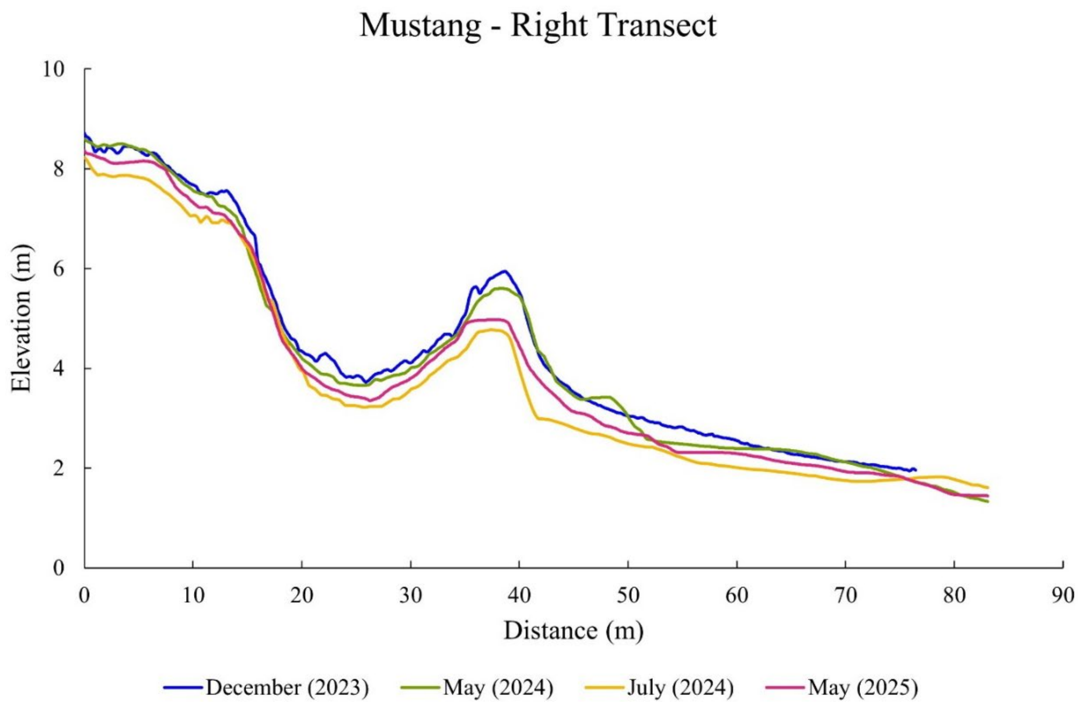

Figure 29. Elevation profiles for Mustang showing changes in elevation of dunes for four DEMs collected in December 2023, May 2024, July 2024, and May 2025. Location of profile shown in Figure 27.

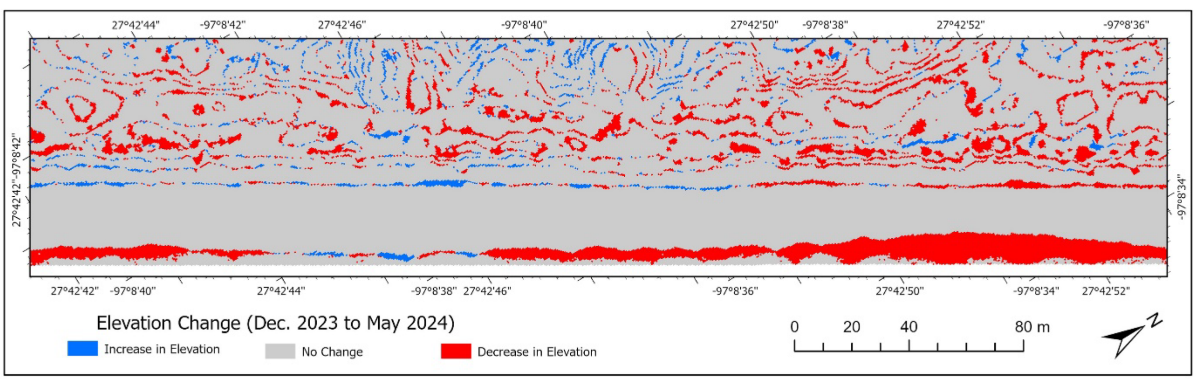

Figure 30. Map of elevation changes between December 2023 and May 2024 for Mustang.

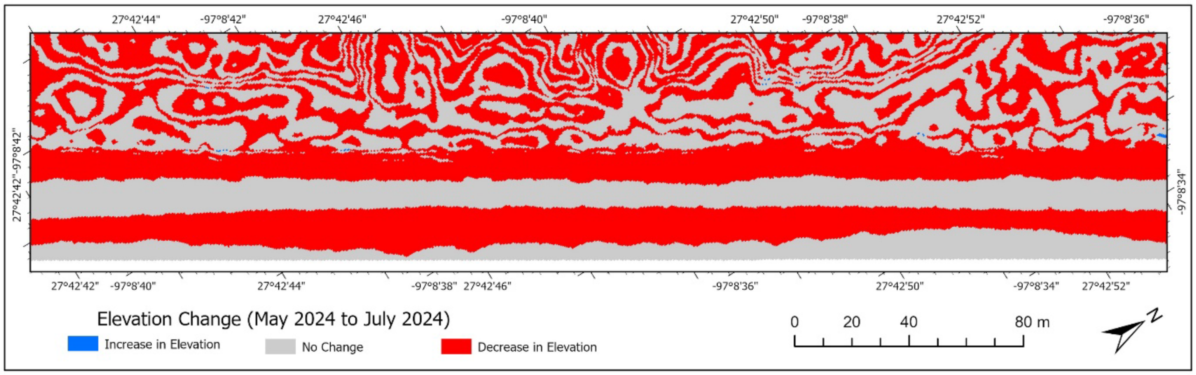

Figure 31. The elevation changes between May 2024 and July 2024 for Mustang.

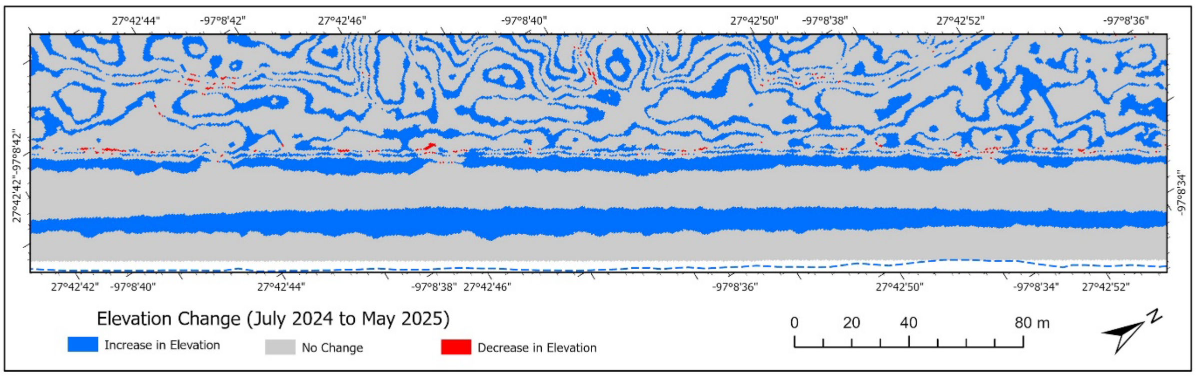

Figure 32. Map of elevation changes between July 2024 and May 2025 for Mustang.

Table 5. Summary of Volume Change for Mustang.

Mustang	December 2023 to May 2024	May 2024 to July 2024	July 2024 to June 2025
Net Gain (m^3)	-1191.2	-21.2	-11195.4
Net Loss (m^3)	5100.2	23105.8	78.7
Net Change (m^3)	3909.0	23084.6	-11116.7
Site Area (m^2)	41233.5	41102.0	41404.7

3.1.6. North Padre Island

Figure 33 displays a DEM image of North Padre Island, collected in June 2025, and it illustrates the vertical and horizontal positions of the dunes. The two red lines on Figure 33 indicate the locations of elevation profiles generated using DEM data from December 2023, May 2024, July 2024, and June 2025 and displayed in Figures 34 and 35.

The left transect in Figure 34 indicates that elevations were almost the same, and the areas were less impacted by Hurricane Beryl. The profile observed in July 2025 shows that the foredunes appear to be rebuilding. The right transect of elevation profiles shown in Figure 35 indicates that the highest elevation was recorded in May 2024, while the most recent DEM shows recovery after erosion by Hurricane Beryl in July 2024.

Figure 36 illustrates the change in elevation between December 2023 and May 2024, indicating an increase in elevation across all areas. Figure 37 highlights the effects of Hurricane Beryl on the beach and the interdunal troughs, demonstrating erosion. The DEM difference between July 2024 and May 2025 shows the recovery and repositioning of sand in areas that were eroded by the hurricane (Figure 38).

Table 6 summarizes the changes in sediment volume. The net volume change between December 2023 and May 2024 is estimated to be 9,863 cubic meters of sediment gain. From May 2024 to July 2024, there is an overall loss of 2,328 cubic meters. However, between July 2024 and June 2025, there is a net loss of 1,878 cubic meters of sediment.

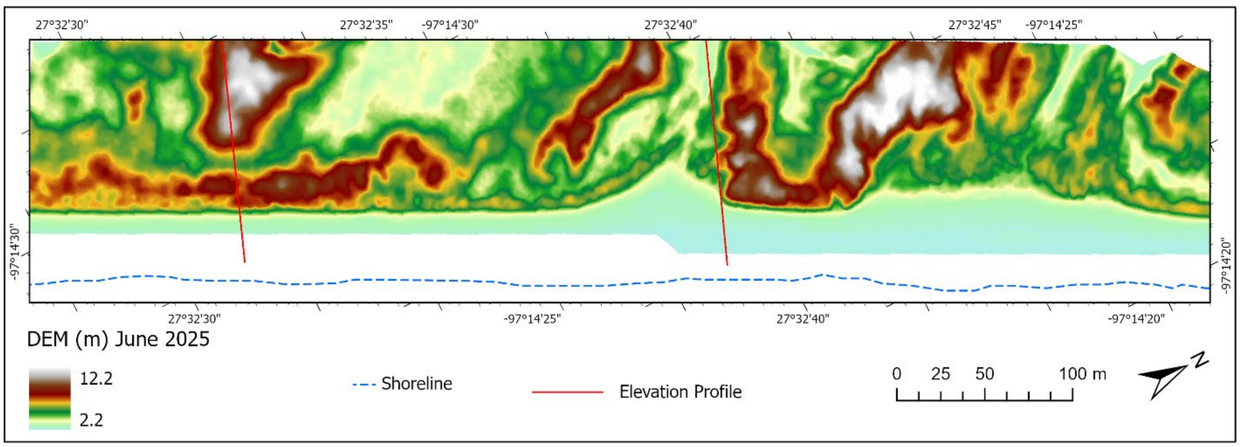

Figure 33. Map depicting the location of profiles and shoreline as of May 2025, DEM. The red line represents the profiles used to create the elevation profiles shown in Figures 34 and 35.

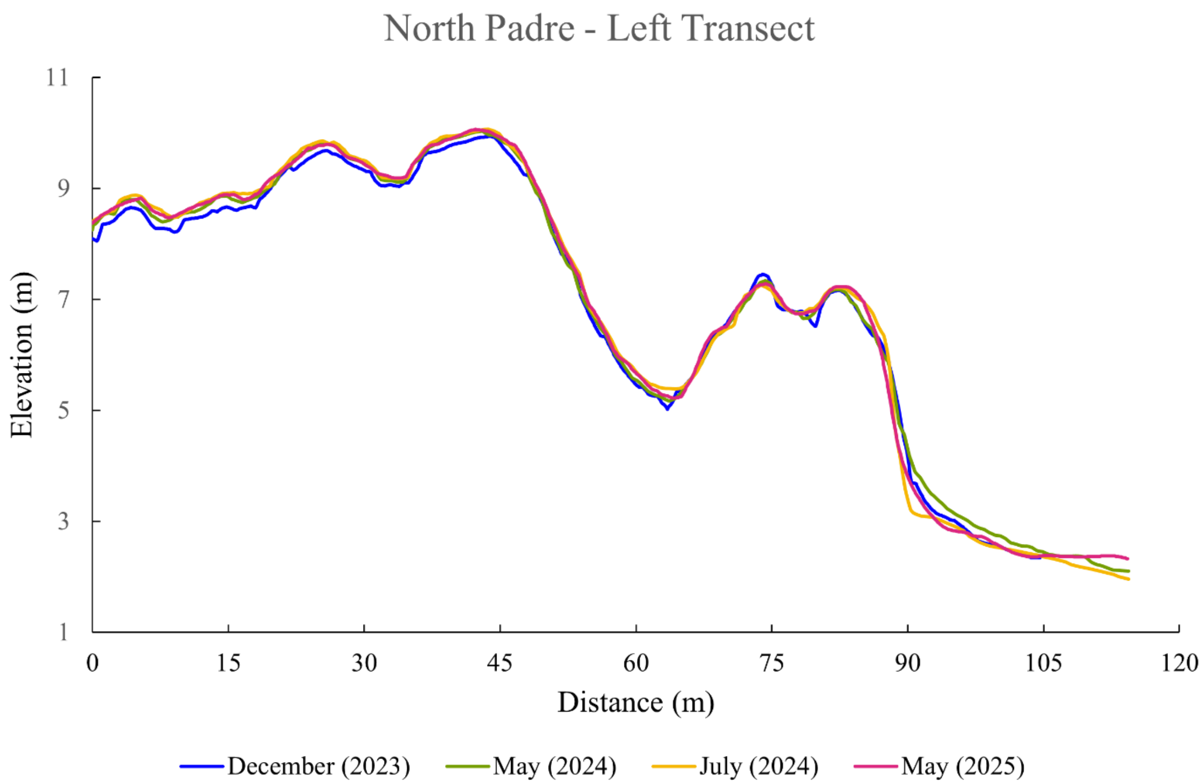

Figure 34. Elevation profiles for North Padre showing changes in elevation of dunes for four DEMs collected in December 2023, May 2024, July 2024, and May 2025. Location of profile shown in Figure 33.

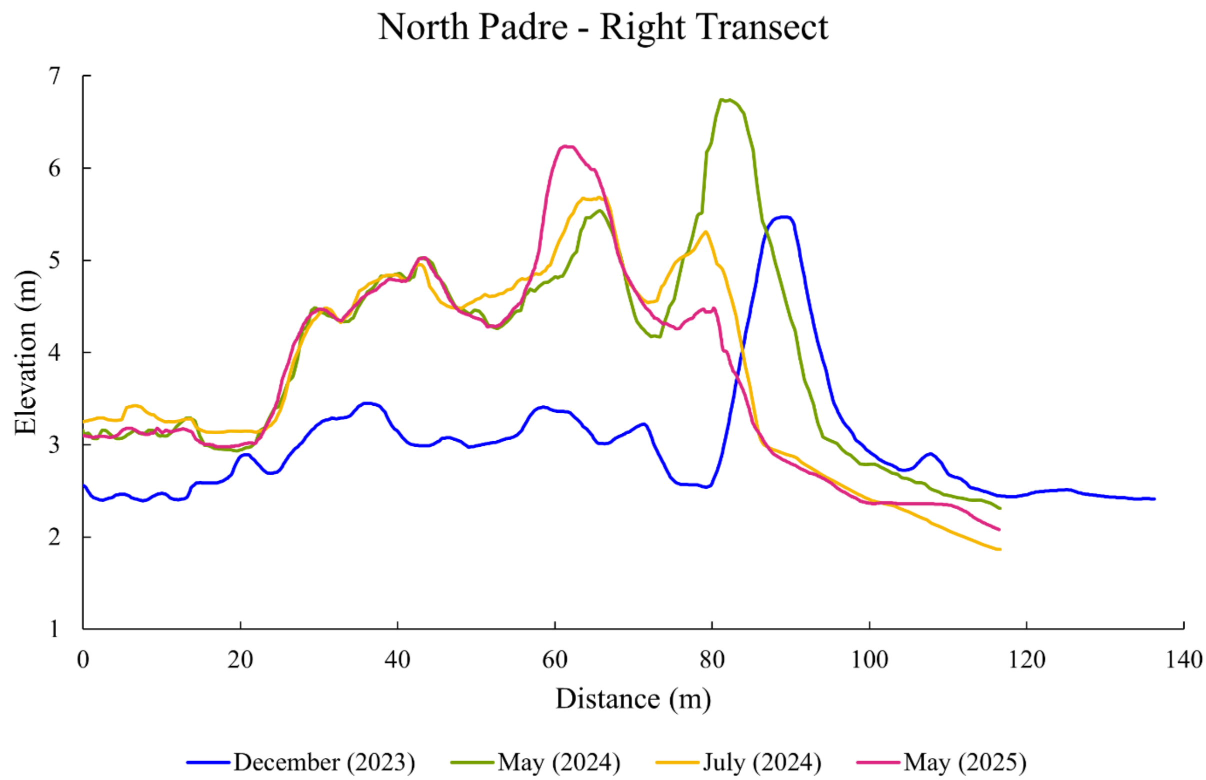

Figure 35. Elevation profiles for North Padre showing changes in elevation of dunes for four DEMs collected in December 2023, May 2024, July 2024, and May 2025. Location of profile shown in Figure 33.

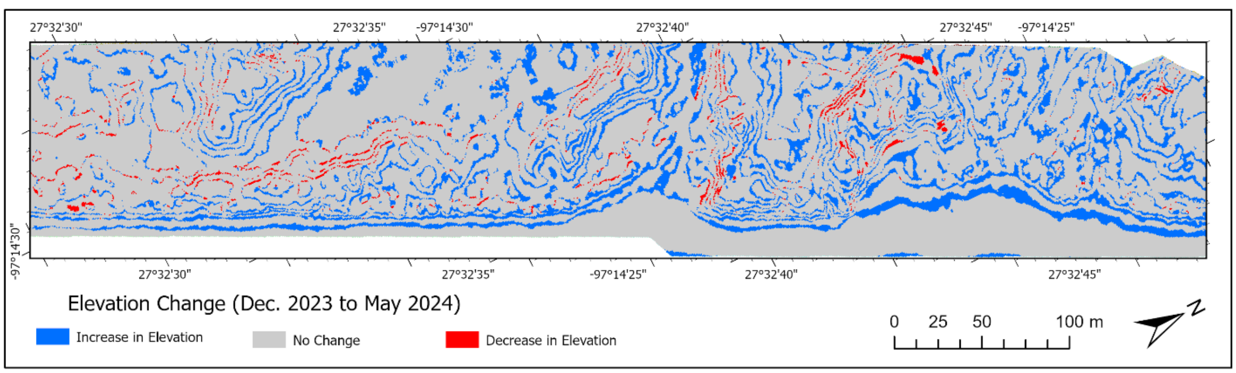

Figure 36. Map of elevation changes between December 2023 and May 2024 for North Padre.

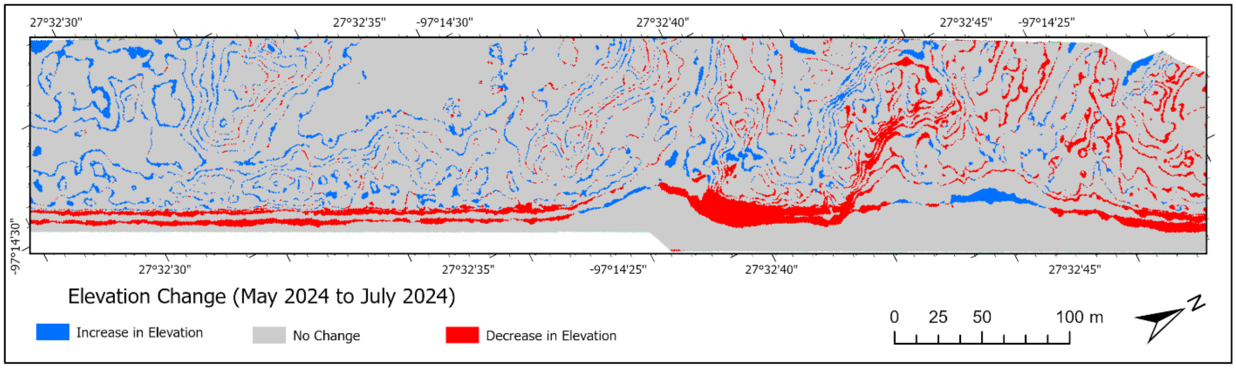

Figure 37. The elevation changes between May 2024 and July 2024 for North Padre.

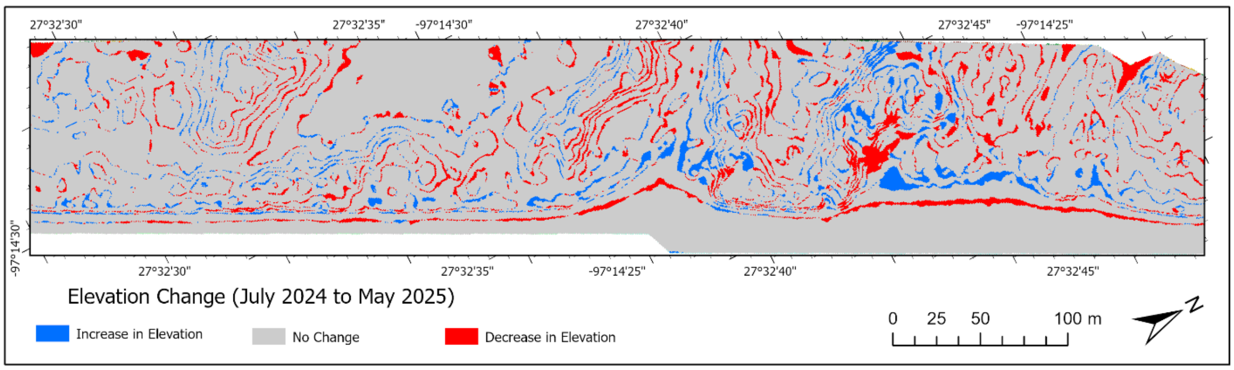

Figure 38. Map of elevation changes between July 2024 and May 2025 for North Padre.

Table 6. Summary of Volume Change for North Padre.

Mustang	**December 2023 to May 2024**	**May 2024 to July 2024**	**July 2024 to June 2025**
Net Gain (m^3)	-10938.0	-3731.0	-3043.0
Net Loss (m^3)	1074.8	6059.8	4921.0
Net Change (m^3)	-9863.3	2328.8	1878.0
Site Area (m^2)	70202.8	70215.8	70181.0

3.2 Time Series Map of Vegetation Change

3.2.1. Galveston

Multispectral drone data were used to construct four maps that show the density of vegetation. For every dataset, NDVI was computed, and the resulting NDVI maps were categorized into four groups: dense, sparse, moderate, and no vegetation. The classified vegetation for December 2023 is shown in Figure 39, with a few isolated patches in other places and numerous densely vegetated areas in the upper left. While the lower portion of the May 2024 image displays little to no vegetation, the top portion displays a sizable area covered in dense vegetation, especially on the coppice dunes (Figure 40).

The map of classified vegetation after Hurricane Beryl is shown in Figure 41. There are now only a few little areas of dense vegetation remaining after most of it was removed. The upper left and a few other spots in the back dune area have extensive vegetation as seen in the most recent vegetation map of June 2025 (Figure 42).

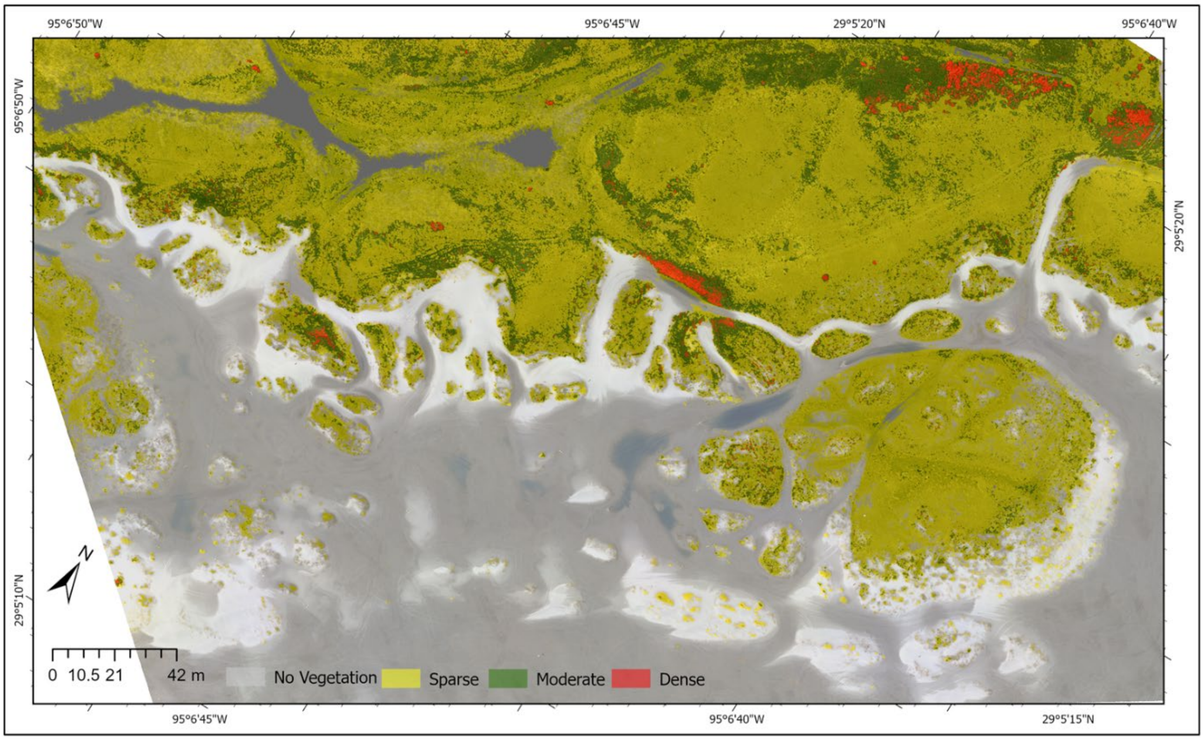

Figure 39. NDVI Classified Images of Galveston for December 2023.

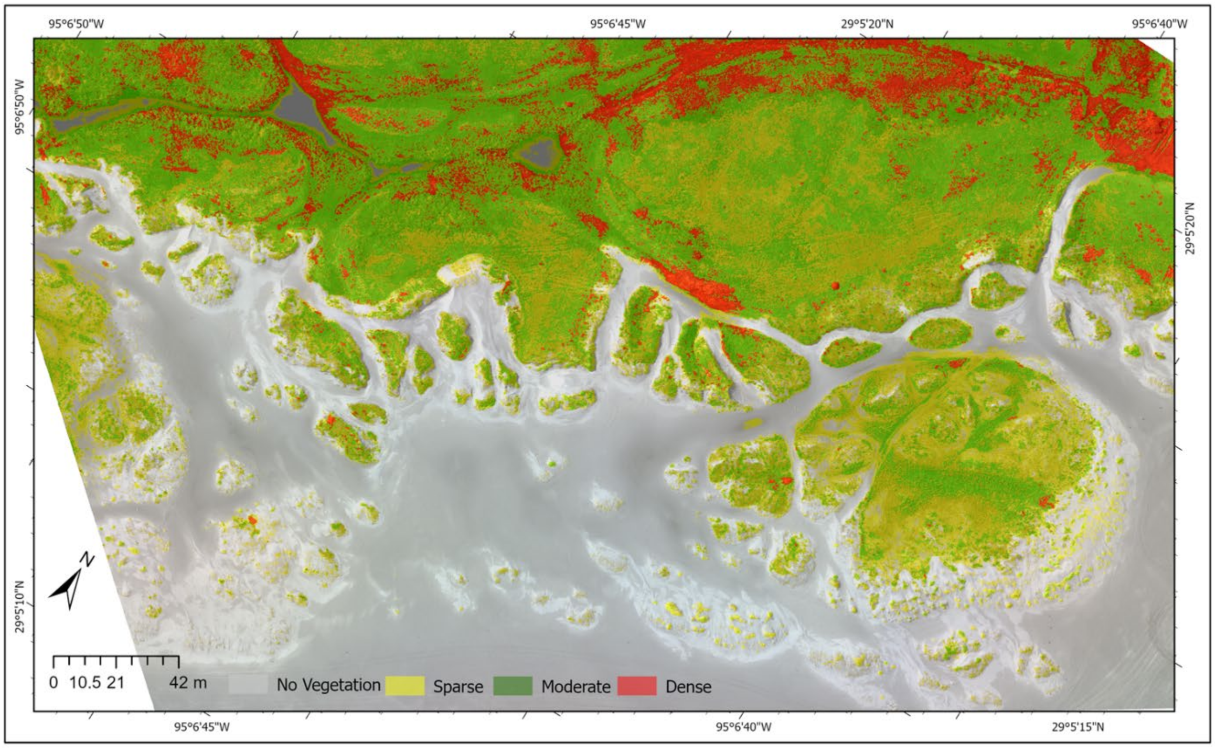

Figure 40. NDVI Classified Images of Galveston for May 2024.

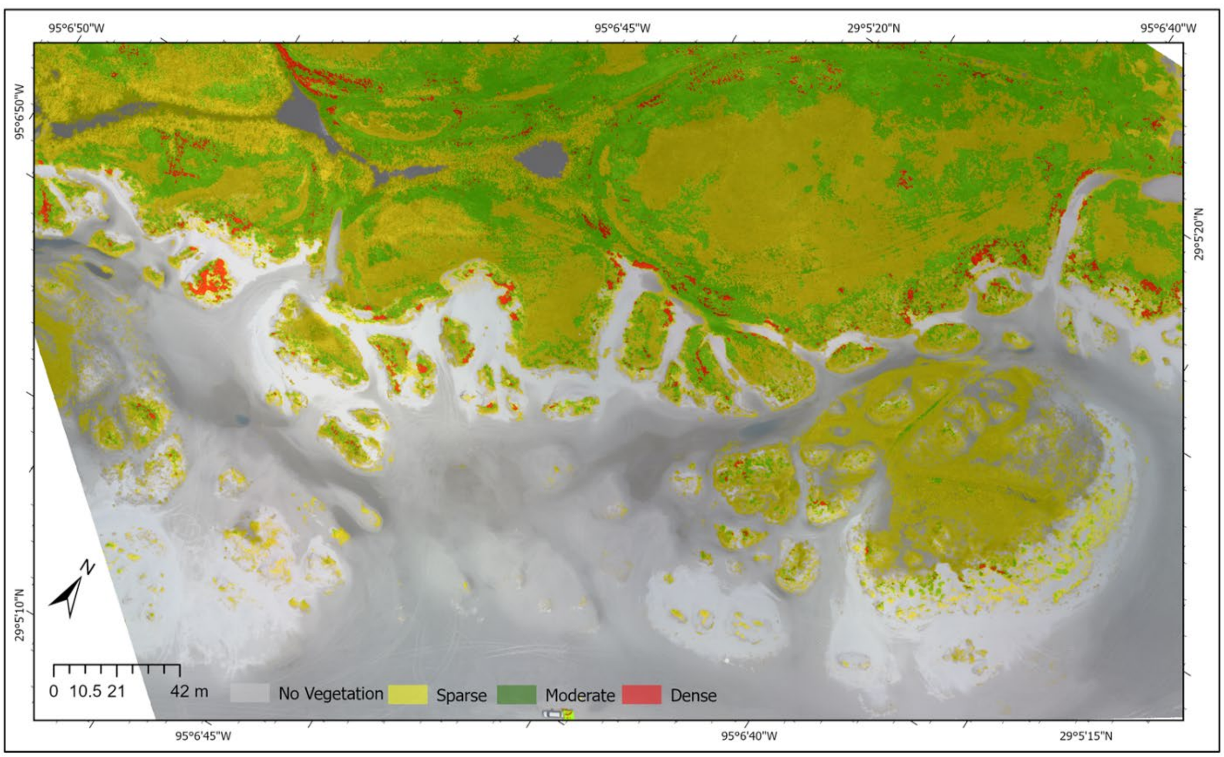

Figure 41. NDVI Classified Images of Galveston for July 2024.

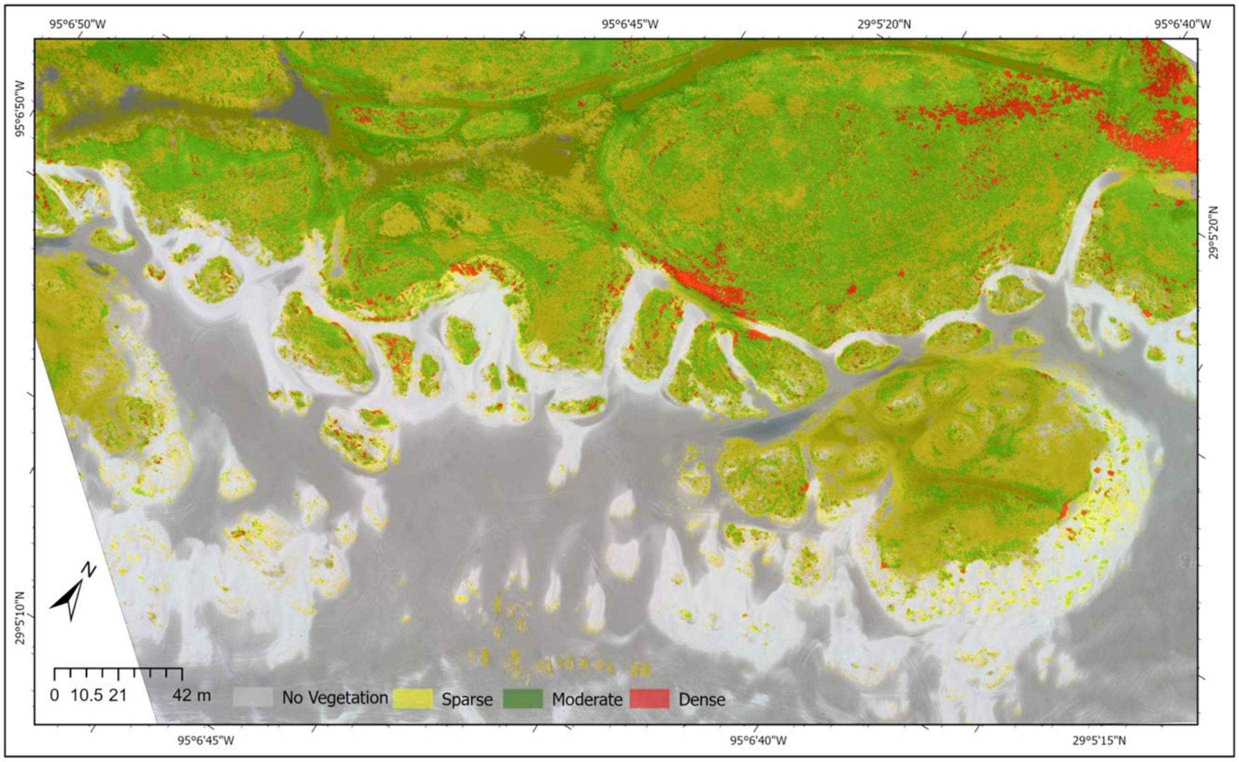

Figure 42. NDVI Classified Images of Galveston for June 2025.

3.2.2. Follet Island

Figure 43 displays the classified vegetation for December 2023, with a few isolated patches of dense vegetation. The map for May 2024 indicates a large area with dense vegetation in the center, as well as many other locations (Figure 44). Figure 45 presents the classified vegetation map following Hurricane Beryl. Most of the dense vegetation has been removed and replaced with areas of sparse or no vegetation, leaving only a few small patches of dense vegetation. The most recent vegetation map from June 2025 shows dense vegetation in most of the area with dunes (Figure 46).

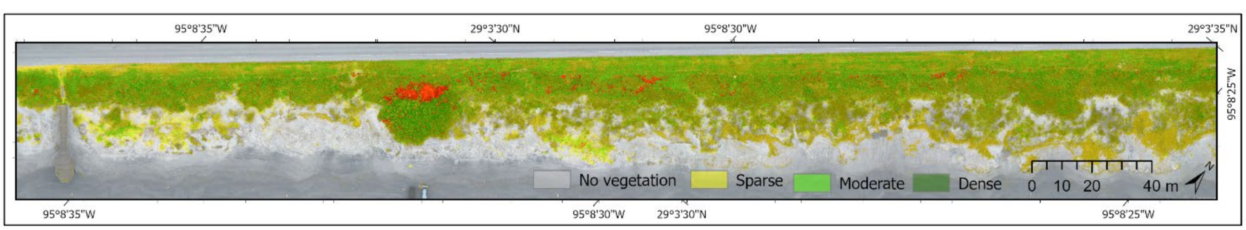

Figure 43. NDVI Classified Images of Follet for December 2023.

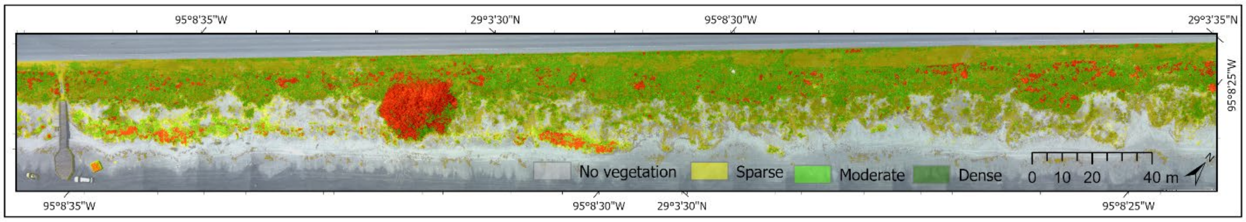

Figure 44. NDVI Classified Images of Follet for May 2024.

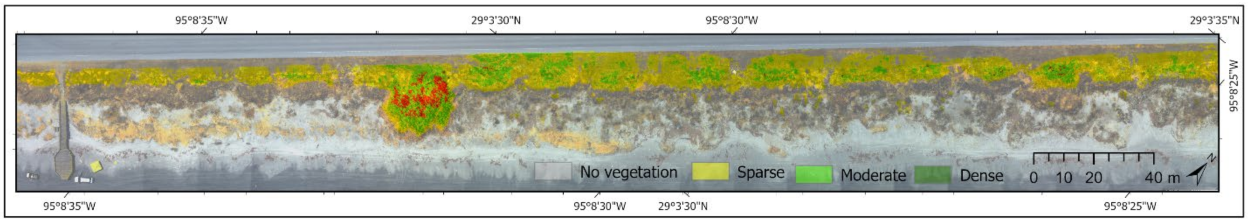

Figure 45. NDVI Classified Images of Follet for July 2024.

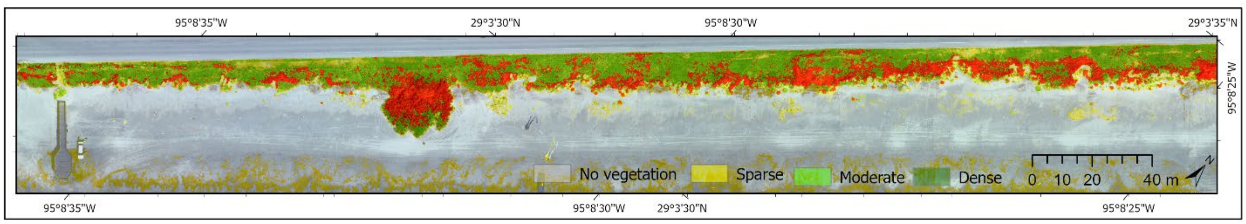

Figure 46. NDVI Classified Images of Follet for June 2025.

3.2.3. Sargent Beach

The classified vegetation for December 2023 is shown in Figure 47, where dense vegetation is only present in a few isolated patches of wetlands. The May 2024 map reveals poor or no vegetation at the bottom, and a small area within the center and to the east, mostly on the coppice dunes (Figure 48). The post-Hurricane Beryl classified vegetation map is shown in Figure 49. Most of the vegetation was removed and replaced by areas of no vegetation. The most recent image of June 2025 shows even less vegetation but shows a few areas where sparse and moderate vegetation is replaced by dense vegetation (Figure 50).

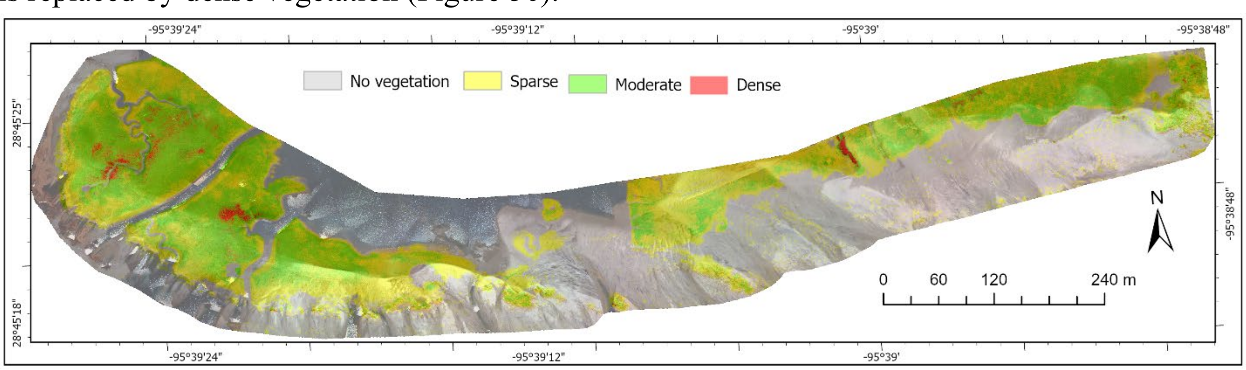

Figure 47. NDVI Classified Images of Sargent for December 2023.

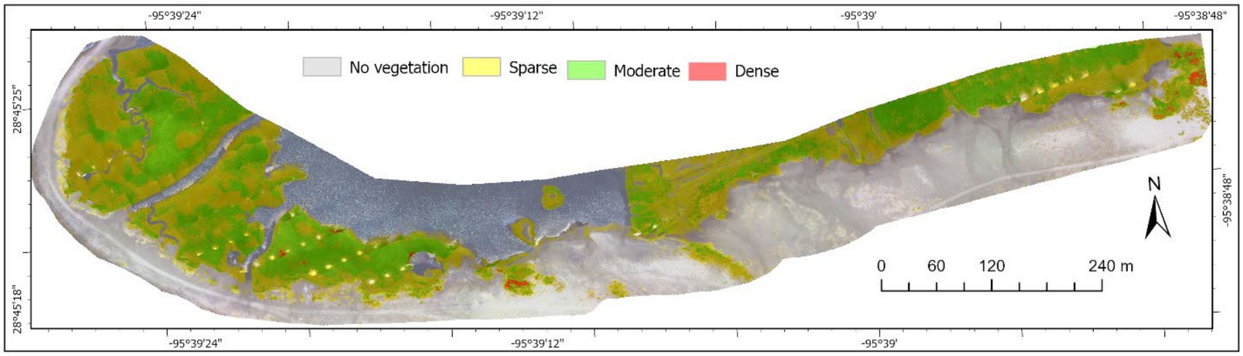

Figure 48. NDVI Classified Images of Sargent for May 2024.

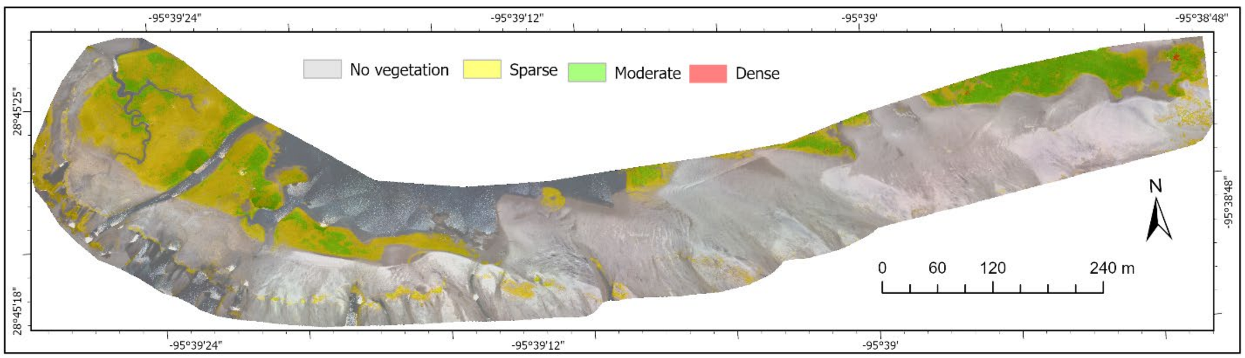

Figure 49. NDVI Classified Images of Sargent for July 2024.

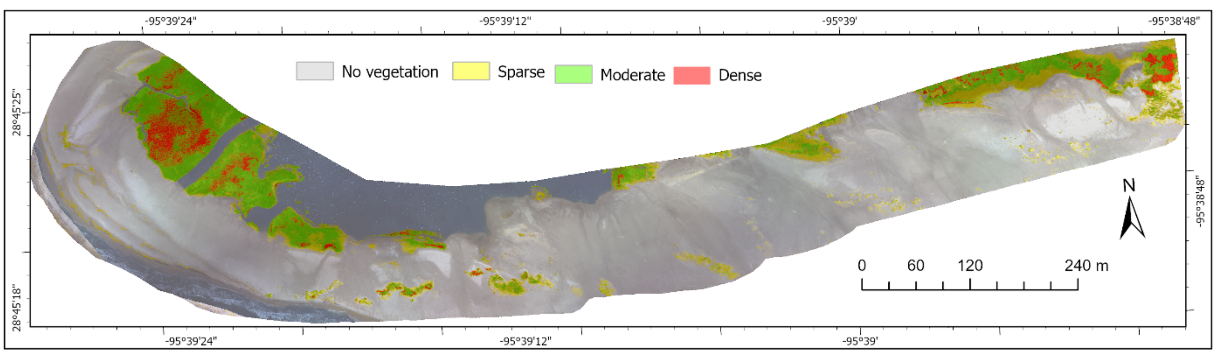

Figure 50. NDVI Classified Images of Sargent for June 2025.

3.2.4. Matagorda Peninsula

The classified vegetation for December 2023 is shown in Figure 51. Most of the dunes are covered by sparse or moderate vegetation. In the May 2024 image, most of the beach and foredunes appear with no vegetation, likely due to recent wind-blown sand being deposited in these areas. However, the back dune region exhibits moderate to dense vegetation, particularly in the top left portion of Figure 52. The post-hurricane image of July 2024 shows more vegetation compared to the May 2024 image (Figure 53). While the most recent image shows most of the area covered by sparse or moderate vegetation, there are also patches of dense vegetation (Figure 54)

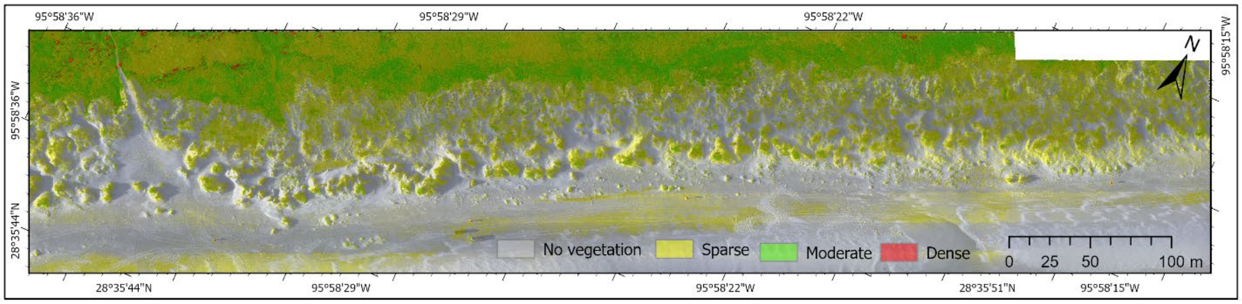

Figure 51. NDVI Classified Images of Matagorda for December 2023.

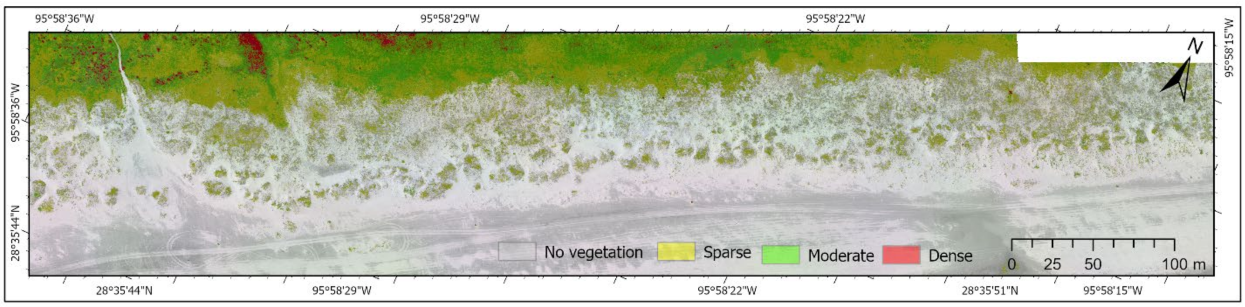

Figure 52. NDVI Classified Images of Matagorda for May 2024.

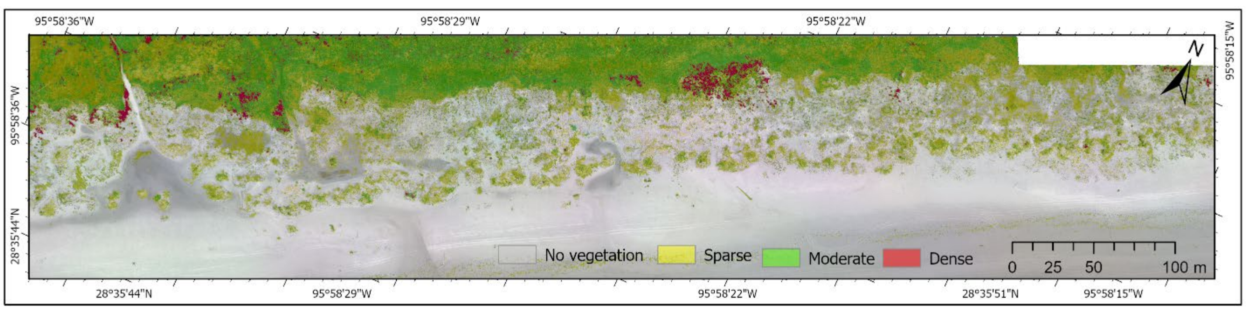

Figure 53. NDVI Classified Images of Matagorda for July 2024.

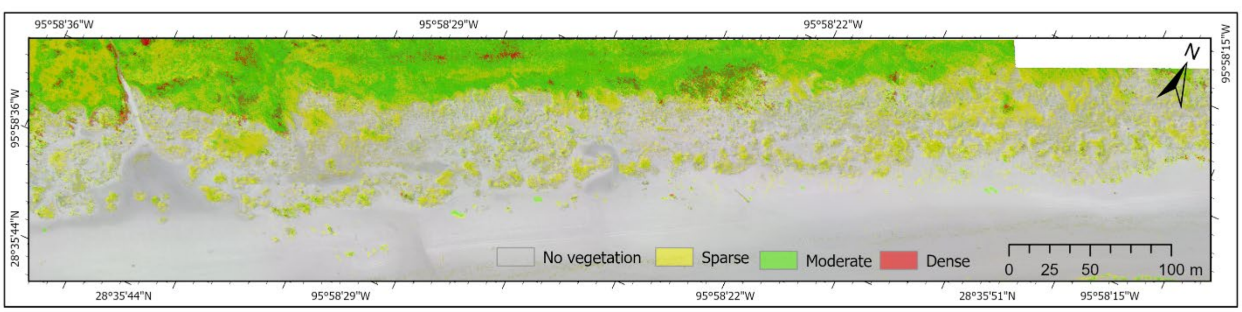

Figure 54. NDVI Classified Images of Matagorda for June 2025.

3.2.5. Mustang Island

December 2023 classified vegetation is shown in Figure 55, where small patches of dense vegetation are present in a number of locations. While most of the dunes are covered by moderate or sparse vegetation (Figure 55). Images collected in summer months show a lot more area covered by dense and moderate vegetation (Figures, 56, 57 and 58).

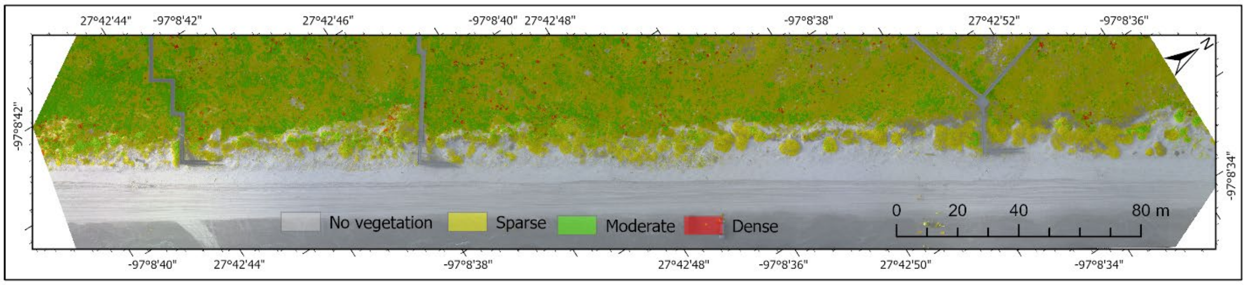

Figure 55. NDVI Classified Images of Mustang for December 2023.

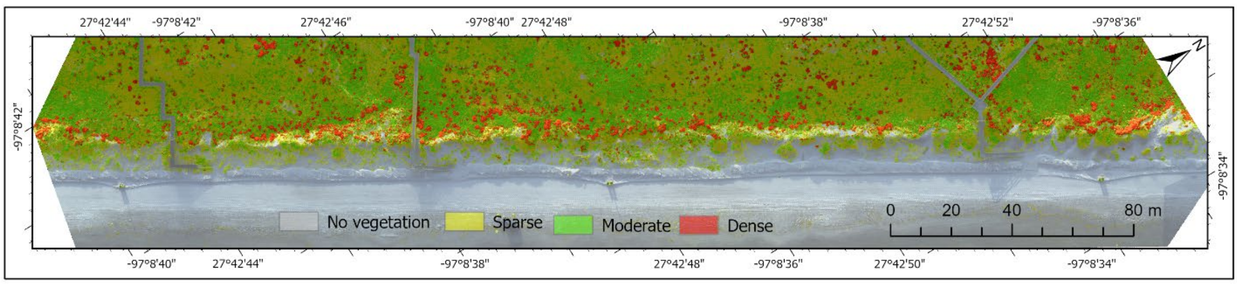

Figure 56. NDVI Classified Images of Mustang for May 2024.

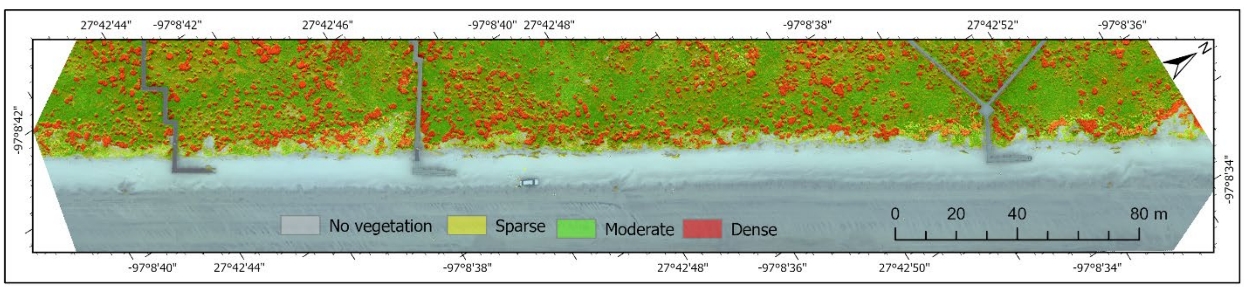

Figure 57. NDVI Classified Images of Mustang for July 2024.

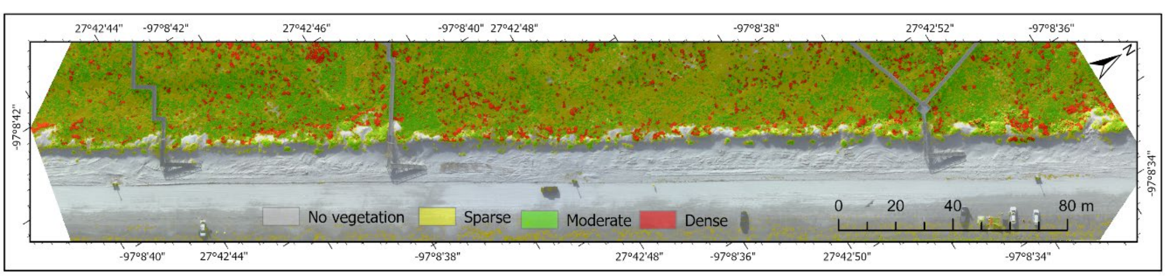

Figure 58. NDVI Classified Images of Mustang for June 2025.

3.2.6. North Padre Island

Figure 59 displays the classified vegetation for December 2023, with very small areas showing dense vegetation. The map for May 2024 indicates the same trend as December 2023, while the bottom section shows sparse or no vegetation (Figure 60).

Figure 61 presents the classified vegetation map following Hurricane Beryl. Most of the dense vegetation has increased. The most recent vegetation map from June 2025 shows dense vegetation and a few other locations in the back dune area (Figure 62).

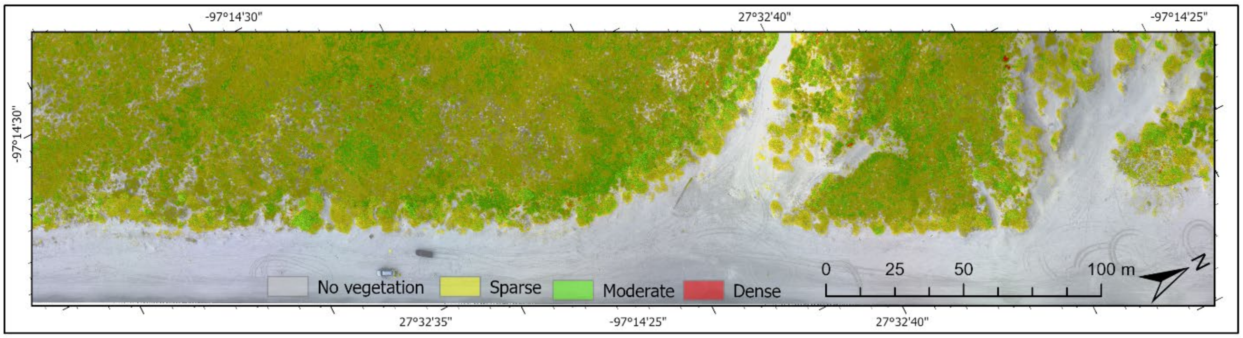

Figure 59. NDVI Classified Images of North Padre for December 2023.

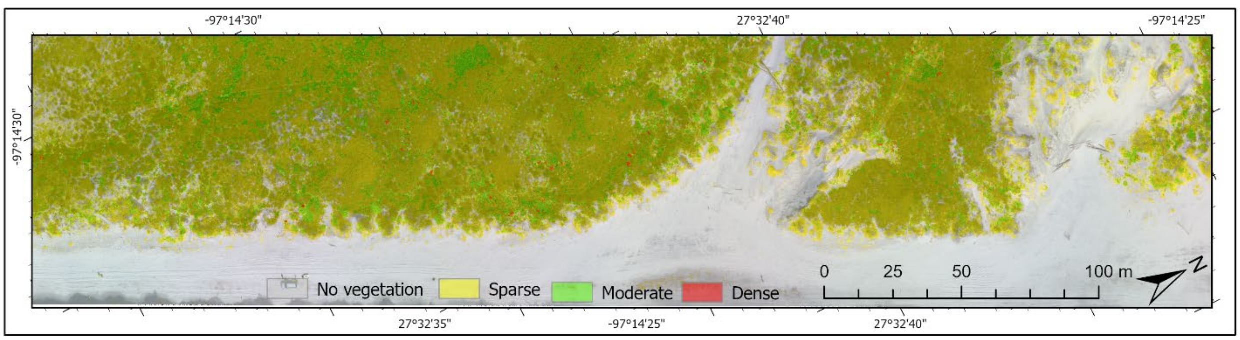

Figure 60. NDVI Classified Images of North Padre for May 2024.

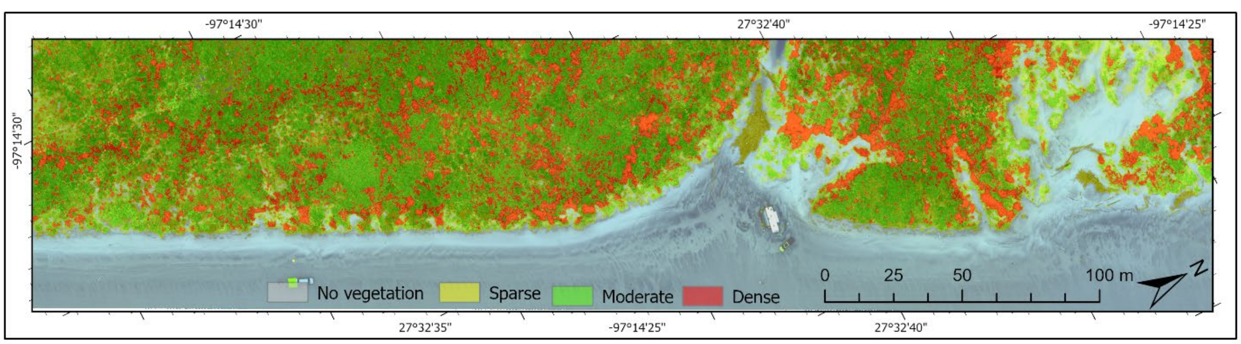

Figure 61. NDVI Classified Images of North Padre for July 2024.

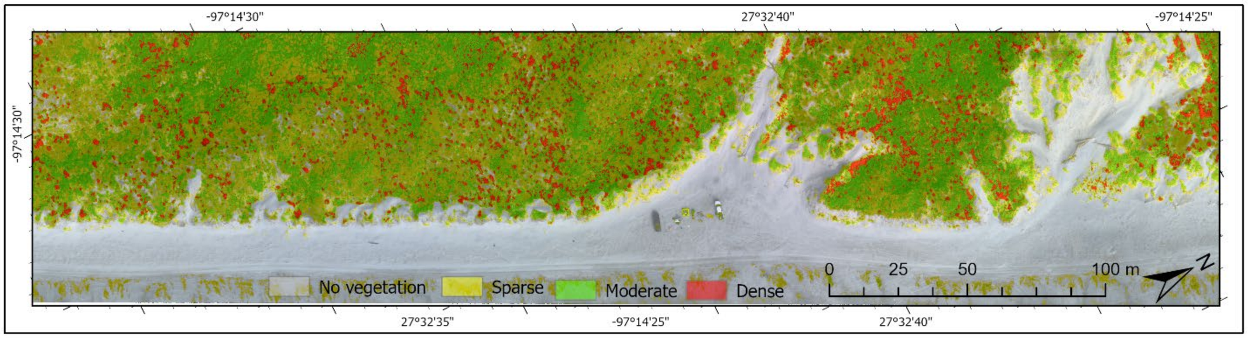

Figure 62. NDVI Classified Images of North Padre for June 2025.

3.3 Website (Story Map)

A website has been created for this project and is hosted on the University of Houston server http://easd.geosc.uh.edu/coastal-erosion/. This website provides a summary of the project and outlines the various techniques employed. Using ESRI Story Maps tools, we have also added an interactive map that includes an orthoimage and Digital Elevation Model (DEM) for each site surveyed during four campaigns: December 2023, May 2024, July/August 2024, and May/June 2025.

3.4 Publication/Outreach

The following peer-reviewed papers and theses resulted from this work.

1. Khan, S.D., Shahtakhtinskiy, A., Younas, M., Garcia, M., Collier, L., Leslie, M., Greer, P., Simon, N. and Karaca, O., 2025. Impact of Hurricane Beryl on Texas beach-dune systems: Insights from drone-based LiDAR and multispectral surveys. Science of The Total Environment, 976, p.179319.
2. Khan, S. D., Erosion Caused by Hurricane Beryl on Texas Barrier Islands: Insights from Drone Surveys. 2025 TxDOT ENV Conference
3. Saidy, C., Khan, S. D., 2025. Effect of Hurricanes on Vegetation and Coastal Erosion at Texas Coastal Sand Dunes, Geological Society of America Zavala Abstracts with Programs 2025
4. LaRochelle, S., Khan, S.D., in revision. Drone-based Multispectral Imagery for Vegetation Density and Classification on the Texas Coast. Journal of Coastal Research

The following thesis and a chapter in the dissertation used data from this project

Simon, N. R., 2024. Remote Sensing Analysis of Beach-Dune Evolution and Identification of Areas at Risk on Central Texas Barrier Islands. M.S Geophysics Thesis, University of Houston

Tirmizi, S. O. A., 2024. Application of Remote Sensing Techniques for the Study of Neotectonic Deformation, Subsidence and Coastal Processes. PhD dissertation University of Houston

In addition, the master's thesis by Leo Collier is scheduled for completion in Fall 2025.
Monitoring Seasonal and Anthropogenic Coastal Change on Matagorda Peninsula through UAV Surveys and Satellite Imagery

Following Hurricane Beryl, several media outlets covered our ongoing research, and below are links to some of the interview coverage.

Coastal Erosion

UH Media
UH Moment
ABC National 1
ABC National 2
Chronicle of Houston
NPR's Houston Matters

4. Discussion

Hurricane Beryl provided a chance to analyze erosion and the different factors that contribute to it on the Texas barrier island. We have published our findings and below is a summary of the results as outlined in Khan et al. (2025).

All six locations examined in this study show erosion within the foredune complex region (Figure 63). The findings indicate that Sargent Beach and Follet Island experienced more erosion in the foredune area compared to the other four locations during Hurricane Beryl. Recent data shows that all sites have made substantial recovery from erosion; however, two years is not enough time to assess and determine the long-term equilibrium of dune systems.

Several factors influence erosion on barrier islands during storms, including wind speed, storm surge, vegetation, beach width, dune elevation, distance from landfall, and storm approach angle (Itzkin et al., 2021; Biel et al., 2017; Sallenger, 2000; Seabloom et al., 2013; Stockdon et al., 2006; Houser et al., 2008; Hesp, 2002). We assessed these factors at six locations using data from Hurricane Beryl.

The strongest wind gusts were recorded at Sargent Beach, reaching speeds of 129 to 161 km/h, accompanied by a 1-meter storm surge (Figure 63). At West Galveston and Follet's Island, storm surges exceeded 1.25 meters, with wind gusts ranging from 113 to 129 km/h. Matagorda Peninsula experienced surges of about 0.9 meters and gusts of 129 to 145 km/h. In contrast, Mustang and North Padre Islands had a storm surge of only 0.37 meters and slower wind gusts of 56 to 64 km/h.

Figure 64 illustrates the different factors affecting erosion in the foredune complex region, such as average beach width, average dune height, vegetation cover, storm surge, wind gusts, distance to landfall, and the storm's side. Typically, areas situated on the right-front quadrant of Hurricane Beryl suffered more erosion, suggesting a more immediate effect in these spots. Mustang Island and North Padre Island were located farthest from the hurricane's landfall along the curved Texas coastline and were oriented at an angle to the storm's trajectory. A notable correlation was found between storm surges and wind gusts; Sargent Beach, Follet's Island, and West Galveston faced significantly greater wind gusts and storm surges, leading to severe erosion compared to the other three sites. Nonetheless, Mustang Island and Matagorda Peninsula were exceptions to this pattern.

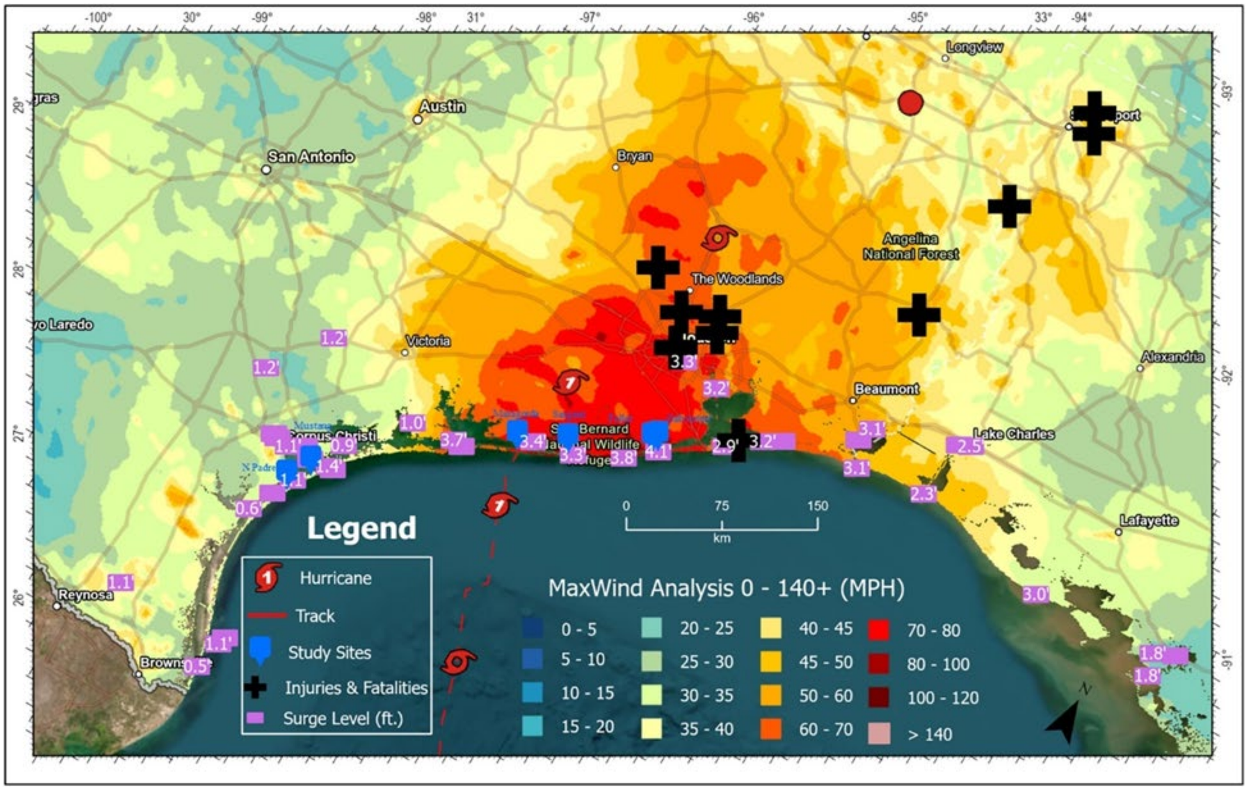

Figure 63. Storm surge and wind gusts from Hurricane Beryl. MPH = Miles per hour. Source of data: NWS GIW NOAA, 2024a, NWS GIW NOAA, 2024b.

The density of vegetation plays a crucial role in mitigating erosion caused by storm surges (Hesp, 2002). This is evident for five out of the six sites examined. For instance, in May, Sargent Beach had 66% of its area lacking vegetation, while only 16% exhibited moderate to dense vegetation. Follett's Island reflected similar findings, with 60% of the area devoid of vegetation and 24% displaying moderate to dense coverage. Conversely, North Padre Island and Mustang Island experienced reduced erosion, with 40% and 22% of their areas free from vegetation and 23% and 33% showing moderate to dense vegetation, respectively. Nevertheless, Matagorda Peninsula stands out as an exception, with 75% of its area without vegetation and only 11% having moderate to dense vegetation.

Beach width has been recognized as a significant factor influencing dune erosion (Itzkin et al., 2021). We also examined it to evaluate the comparative impact of beach width on the resilience of coastal systems during major storms. In May, West Galveston had the most extensive beach at 176 m. This was followed by Matagorda Peninsula at 68 m, North Padre Island at 29 m, Mustang Island at 21 m, Follet's Island at 15 m, and Sargent Beach at 8 m. Erosion was most severe at Sargent Beach and Follet's Island, which also had the narrowest beach widths. This could have played a role in the erosion experienced at these two locations.

The height of dunes has a strong correlation with the extent of damage and erosion they experience (Houser et al., 2008; Hesp, 2002). For example, the highest dunes were located at North Padre Island (average elevation of 5.7 m) and Mustang Island (average elevation of 4.3 m), both of which experienced less damage. In contrast, the lowest average dune elevations were found at Sargent Beach (2.3 m), Follet's Island (3.5 m), and West Galveston (3.3 m), all of which experienced significant damage. Meanwhile, Matagorda Peninsula had an intermediate average dune elevation of 3.7 m and saw less damage overall. Similar patterns were observed on the central and upper Texas coast after Hurricane Harvey (2017), where sites with taller foredunes acted as barriers, attenuating wave energy and storm surge impacts, resulting in reduced overwash and scarping (Shahtakhtinskiy et al., 2023; Rojas et al., 2022).

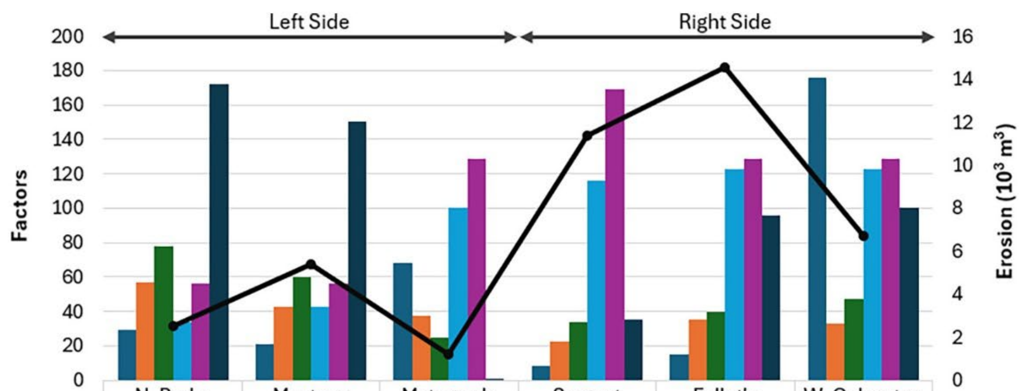

	N. Padre	Mustang	Matagorda	Sargent	Follet's	W. Galveston
Average Beach Width (m)	29	21	68	8	15	176
Average Dune Height (dm)	56.7	42.8	37.4	22.9	35.4	33
Vegetation Cover (%)	78	60	25	34	40	47
Storm Surge (cm)	34	43	100	116	123	123
Wind Gust (km/h)	56	56	129	169	129	129
Distance to landfall (km)	172	150	0.75	35	96	100
Foredune Area Erosion ($10^3 m^3$)	2.5	5.4	1.2	11.4	14.6	6.7

Figure 64. Summary of the factors influencing erosion and storm impact at the six studied sites.

5. Conclusion

This research used high-resolution remote sensing data to assess the geological impacts of a major storm on six key locations along the Texas Gulf Coast. During this study, Hurricane Beryl caused billions of dollars in damage to coastal dunes and beach systems. The hurricane resulted in flooding, destruction from high winds, transportation disruptions, and prolonged power outages in Houston and nearby areas, affecting millions of homes and businesses.

Implications for Future Management of the Texas Coast

This research highlights the importance and effectiveness of capturing high-resolution drone imagery and topographic data immediately before and after a major storm event to assess its immediate impact on beach-dune systems. These insights are crucial for understanding erosion trends and enhancing dune resilience for coastal protection.

The study found that dunes lacking sufficient height or vegetation were more susceptible to erosion and breaches, particularly noted at Sargent Beach and Follet's Island. Additionally, the width of the beach appears to have influenced the extent of the damage observed. To mitigate storm impacts and reduce erosion, it is recommended to maintain or increase dune height and vegetation cover.

References

National Oceanic and Atmospheric Administration, pp. 1-3 (accessed February 2, 2025). www.weather.

Baustian, J. J., & Mendelssohn, I. A. (2015). Hurricane-induced sedimentation improves marsh resilience and vegetation vigor under high rates of relative sea level rise. *Wetlands*, *35*(4), 795-802.

Biel, R. G., Hacker, S. D., Ruggiero, P., Cohn, N., & Seabloom, E. W. (2017). Coastal protection and conservation on sandy beaches and dunes: context-dependent tradeoffs in ecosystem service supply. Ecosphere, 8(4), e01791.

Cherry, J. A., McKee, K. L., & Grace, J. B. (2009). Elevated CO2 enhances biological contributions to elevation change in coastal wetlands by offsetting stressors associated with sea-level rise. *Journal of Ecology*, *97*(1), 67-77.

Fabbri, S., Grottoli, E., Armaroli, C., & Ciavola, P. (2021). Using high-spatial resolution UAV-derived data to evaluate vegetation and geomorphological changes on a dune field involved in a restoration endeavour. *remote sensing*, *13*(10), 1987.

Feagin, R. A., Figlus, J., Zinnert, J. C., Sigren, J., Martínez, M. L., Silva, R., ... & Carter, G. (2015). Going with the flow or against the grain? The promise of vegetation for protecting beaches, dunes, and barrier islands from erosion. *Frontiers in Ecology and the Environment*, *13*(4), 203-210.

Feagin, R. A., Furman, M., Salgado, K., Martinez, M. L., Innocenti, R. A., Eubanks, K., ... & Silva, R. (2019). The role of beach and sand dune vegetation in mediating wave run up erosion. *Estuarine, Coastal and Shelf Science*, *219*, 97-106.

Finley, R. J. (1976). Interpretation of unenhanced Landsat imagery for wetland and land use delineation in the Texas coastal zone.

Hallam, S., Marsh, R., Josey, S. A., Hyder, P., Moat, B., & Hirschi, J. J. M. (2019). Ocean precursors to the extreme Atlantic 2017 hurricane season. *Nature communications*, *10*(1), 896.

Hesp, P. (2002). Foredunes and blowouts: initiation, geomorphology and dynamics. Geomorphology, 48(1-3), 245-268.

Holland, G. J., & Webster, P. J. (2007). Heightened tropical cyclone activity in the North Atlantic: natural variability or climate trend?. *Philosophical Transactions of the Royal Society A: Mathematical, Physical and Engineering Sciences*, *365*(1860), 2695-2716.

Houser, C., Hapke, C., & Hamilton, S. (2008). Controls on coastal dune morphology, shoreline erosion and barrier island response to extreme storms. Geomorphology, 100(3-4), 223-240.

Itzkin, M., Moore, L. J., Ruggiero, P., Hacker, S. D., & Biel, R. G. (2021). The relative influence of dune aspect ratio and beach width on dune erosion as a function of storm duration and surge level. Earth Surface Dynamics, 9(5), 1223-1237.

Khan, S.D., Shahtakhtinskiy, A., Younas, M., Garcia, M., Collier, L., Leslie, M., Greer, P., Simon, N. and Karaca, O., (2025). Impact of Hurricane Beryl on Texas beach-dune systems: Insights from drone-based LiDAR and multispectral surveys. Science of The Total Environment, 976, p.179319.

Maun, M. A. (1998). Adaptations of plants to burial in coastal sand dunes. *Canadian journal of botany*, *76*(5), 713-738.

Morton, R. A., & Paine, J. G. (1990). Coastal Land Loss in Texas--An Overview.

NWS GIW NOAA, 2024a. Hurricane Beryl Estimated Maximum Wind Gusts. https://www.arcgis.com/apps/mapviewer/index.html?basemapUrl=https://tiles.arcgis.com/tiles/C8EMgrsFcRFL6LrL/arcgis/rest/services/REGION_6_MaxWindAnalysis_07062024_0800PM_07082024_0800PM_EDT_Image/MapServer?cacheKey=a0c491acb447cbf1 Accessed January 3, 2025.

NWS GIW NOAA, 2024b. 202407 Beryl NWS preliminary reports - surge level https://www.arcgis.com/apps/mapviewer/index.html?url=https://services6.arcgis.com/LT1iWT50Endhh6TU/ArcGIS/rest/services/202407_Beryl_NWS_Preliminary_Reports/FeatureServer/5&source=sd accessed January 3, 2025.

Paine, J. G., Caudle, T. L., & Andrews, J. (2013). Shoreline, beach, and dune morphodynamics, Texas Gulf Coast.

Rojas, S. S., Khan, S. D., & Shahtakhtinskiy, A. (2022). Impact of hurricane harvey on the upper Texas Coast: Using airborne lidar data sets with UAV-derived topographic data to monitor change and track recovery. *Remote Sensing*, *14*(21), 5357.

Rojas, S. S., Khan, S. D., & Shahtakhtinskiy, A. (2022). Impact of Hurricane Harvey on the upper Texas Coast: Using airborne lidar data sets with UAV-derived topographic data to monitor change and track recovery. Remote Sensing, 14(21), 5357.

Sallenger Jr, A. H. (2000). Storm impact scale for barrier islands. Journal of coastal research, 890-895.

Seabloom, E. W., Ruggiero, P., Hacker, S. D., Mull, J., & Zarnetske, P. (2013). Invasive grasses, climate change, and exposure to storm-wave overtopping in coastal dune ecosystems. Global change biology, 19(3), 824-832.

Shahtakhtinskiy, A., Khan, S. D., & Rojas, S. S. (2023). Quantifying the Impact of Hurricane Harvey on Beach− Dune Systems of the Central Texas Coast and Monitoring Their Changes Using UAV Photogrammetry. Remote Sensing, 15(24), 5779.

Stockdon, H. F., Holman, R. A., Howd, P. A., & Sallenger Jr, A. H. (2006). Empirical parameterization of setup, swash, and runup. Coastal engineering, 53(7), 573-588.

Tsoar, H. (2005). Sand dunes mobility and stability in relation to climate. *Physica A: Statistical Mechanics and its Applications*, *357*(1), 50-56.